CRC Press
Taylor & Francis Group

Diverse Quasiparticle Properties of Emerging Materials

First-Principles Simulations

Edited by Tran Thi Thu Hanh, Vo Khuong Dien, Ngoc Thanh Thuy Tran, Ching-Hong Ho, Thi Dieu Hien Nguyen, and Ming-Fa Lin

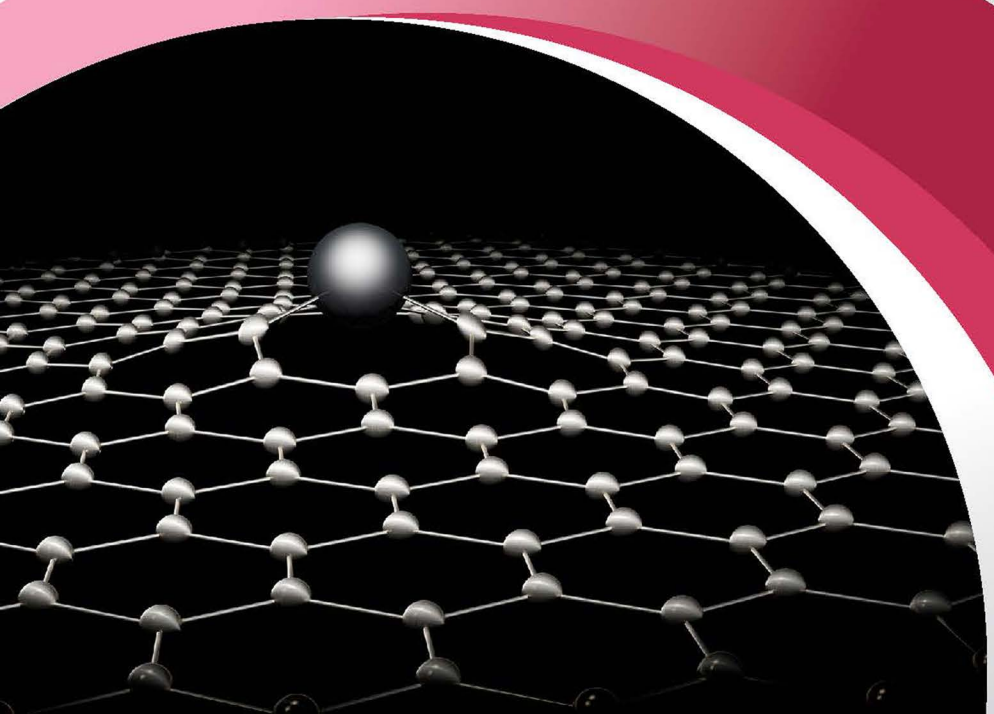

Diverse Quasiparticle Properties of Emerging Materials

Diverse Quasiparticle Properties of Emerging Materials: First-Principles Simulations thoroughly explores the rich and unique quasiparticle properties of emergent materials through a VASP-based theoretical framework. Evaluations and analyses are conducted on the crystal symmetries, electronic energy spectra/wave functions, spatial charge densities, van Hove singularities, magnetic moments, spin configurations, optical absorption structures with/without excitonic effects, quantum transports, and atomic coherent oscillations.

Key Features

- Illustrates various quasiparticle phenomena, mainly covering orbital hybridizations and spin-up/spin-down configurations
- Mainly focuses on electrons and holes, in which their methods and techniques could be generalized to other quasiparticles, such as phonons and photons
- Considers such emerging materials as zigzag nanotubes, nanoribbons, germanene, plumbene, bismuth chalcogenide insulators
- Includes a section on applications of these materials

This book is aimed at professionals and researchers in materials science, physics, and physical chemistry, as well as upper-level students in these fields.

Diverse Quasiparticle Properties of Emerging Materials

First-Principles Simulations

Edited by
Tran Thi Thu Hanh
Vo Khuong Dien
Ngoc Thanh Thuy Tran
Ching-Hong Ho
Thi Dieu Hien Nguyen
Ming-Fa Lin

CRC Press
Taylor & Francis Group
Boca Raton London

CRC Press is an imprint of the
Taylor & Francis Group, an **informa** business

First edition published 2023
by CRC Press
6000 Broken Sound Parkway NW, Suite 300, Boca Raton, FL 33487–2742

and by CRC Press
4 Park Square, Milton Park, Abingdon, Oxon, OX14 4RN

CRC Press is an imprint of Taylor & Francis Group, LLC

ISBN: 978-1-032-32305-3 (hbk)
ISBN: 978-1-032-34519-2 (pbk)
ISBN: 978-1-003-32257-3 (ebk)

DOI: 10.1201/9781003322573

Typeset in Times
by Apex CoVantage, LLC

Contents

Preface

This book *Diverse Quasiparticle Properties of Emerging Materials: First-Principles Simulations* is completed with intensive cooperation in scientific research between research groups from Taiwan and Vietnam. This book comprises 20 comprehensive chapters on the theoretical framework of quasiparticle properties. There are two approaches of quasiparticle viewpoints dominating the theoretical developments, namely, first-principles simulations and phenomenological models. This work is focused on the first-principles simulations.

The calculated results include the total ground state energies/the chemical modification energies, the optimal Moiré superlattices/normal unit cells, the atom- and spin-dominated band structures/wave functions, the spatial charge/spin density distributions, the atom- orbital- and spin-decomposed van Hove singularities, the net magnetic moments, the single-particle and many-body reflectance, absorption, transmission and energy loss spectra, the ballistic electrical conductivities, the Hall quantum ones, and the vibration phonons. They are sufficient to identify the various quasiparticle behaviors and to further generalize the previous theoretical framework.

Most of the research results in this book are carried out by research groups at prestigious universities such as National Cheng Kung University, Taiwan; Ho Chi Minh City University of Technology (HCMUT)—Vietnam National University Ho Chi Minh City, Vietnam; National Kaohsiung University of Science and Technology, Taiwan; Can Tho University, Vietnam; Can Tho University of Medicine and Pharmacy, Vietnam; Thu Dau Mot University, Vietnam. We are grateful to all the authors for their excellent contributions.

This book will hopefully be of great interest to the scientific community, and it will contribute to the development of research of emergent materials.

Acknowledgments

This work was financially supported by the Hierarchical Green-Energy Materials (Hi-GEM) Research Center, from The Featured Areas Research Center Program within the framework of the Higher Education Sprout Project by the Ministry of Education (MOE) and the Ministry of Science and Technology (Grant number MOST 108–2112-M-006–016-MY3) in Taiwan.

Editors

Tran Thi Thu Hanh is a lecturer at the Ho Chi Minh City University of Technology, Vietnam National University, Ho Chi Minh City, Vietnam. Dr. Hanh graduated with bachelor's and master's degrees from Voronezh State University, Russia, and a doctorate from Tokyo University, Japan. Her main area of research is computational physics using molecular dynamics and density functional theory methods. Dr. Hanh focuses on studying the interaction, the hydrogen storage of fuel cells, and the electronic properties, structural deformation of 2D, 3D materials, with many quality articles published in international journals. Find her on the web at https://fas.hcmut.edu.vn/personnel/thuhanhsp.

Vo Khuong Dien is a Ph.D. student at the Department of Physics, National Cheng Kung University. His research interests include the electronic and optical properties of low-dimensional group materials and first-principles calculations.

Ngoc Thanh Thuy Tran obtained her Ph.D. in physics in 2017 from the National Cheng Kung University (NCKU), Taiwan. Afterward, she worked as a postdoctoral researcher and then was promoted to assistant researcher at Hierarchical Green-Energy Materials (Hi-GEM) Research Center, NCKU. Her scientific interest is focused on the fundamental (electronic, magnetic, and thermodynamic) properties of 2D materials and rechargeable battery materials by means of the first-principles calculations.

Ching-Hong Ho is a postdoctoral researcher in the Department of Physics, National Cheng Kung University, Taiwan, where he received his Ph.D. in 2011. His research area of interest is theoretical condensed matter physics with a focus on topological aspects in the past years.

Thi Dieu Hien Nguyen achieved her Ph.D. in physics in July 2021 from National Cheng Kung University (NCKU), Taiwan Currently, she works as a postdoctoral researcher at NCKU. Her academic research focuses on essential properties of 1D, 2D materials and anode, cathode, electrolyte battery materials using first-principles calculations.

Ming-Fa Lin is a distinguished professor in the Department of Physics, National Cheng Kung University, Taiwan. He received his Ph.D. in physics in 1993 from the National Tsing-Hua University, Taiwan. His main scientific interests focus on essential properties of carbon related materials and low-dimensional systems.

Contributors

Vo Duy Dat
Institute of Applied Technology
Thu Dau Mot University
Binh Duong, Vietnam

Vo Khuong Dien
Department of Physics
National Cheng Kung University
Tainan, Taiwan

Nguyen Thi Han
Department of Physics
National Cheng Kung University
Tainan, Taiwan

Tran Thi Thu Hanh
Laboratory of Computational Physics, Faculty of Applied Science
Ho Chi Minh City University of Technology (HCMUT)
Ho Chi Minh City, Vietnam
and
Vietnam National University Ho Chi Minh City
Ho Chi Minh City, Vietnam

Ching-Hong Ho
Department of Physics
National Cheng Kung University
Tainan, Taiwan

Nguyen Van Hoa
Laboratory of Computational Physics, Faculty of Applied Science
Ho Chi Minh City University of Technology (HCMUT)
Ho Chi Minh City, Vietnam
and
Vietnam National University Ho Chi Minh City
Ho Chi Minh City, Vietnam

Thi My Duyen Huynh
Department of Physics
National Cheng Kung University
Tainan, Taiwan

Phuoc Huu Le
Department of Physics and Biophysics, Faculty of Basic Sciences
Can Tho University of Medicine and Pharmacy
Can Tho, Vietnam

Ming-Fa Lin
Department of Physics
National Cheng Kung University
Tainan, Taiwan

Chiun-Yan Lin
Department of Physics
National Cheng Kung University
Tainan, Taiwan

Shih-Yang Lin
Department of Physics
National Cheng Kung University
Tainan, Taiwan

Wei-Bang Li
Core Facility Center
National Cheng Kung University
Tainan, Taiwan

Hsin-Yi Liu
Center for Micro/Nano Science and Technology
National Cheng Kung University
Tainan, Taiwan

Thi Dieu Hien Nguyen
Department of Physics
National Cheng Kung University
Tainan, Taiwan

Duy Khanh Nguyen
Institute of Applied Technology
Thu Dau Mot University
Binh Duong, Vietnam

Vo Van On
Institute of Applied Technology
Thu Dau Mot University
Binh Duong, Vietnam

Jheng-Hong Shih
Department of Physics
National Cheng Kung University
Tainan, Taiwan

Pham Thi Bich Thao
Department of Physics
College of Natural Sciences
Can Tho University
Can Tho, Vietnam

Nguyen Thanh Tien
Department of Physics
College of Natural Sciences
Can Tho University
Can Tho, Vietnam

Ngoc Thanh Thuy Tran
Hierarchical Green-Energy Materials Research Center
National Cheng Kung University
Tainan, Taiwan

Ming-Hsiu Tsai
Department of Physics
National Cheng Kung University
Tainan, Taiwan

Le Thi Cam Tuyen
Department of Chemical Engineering, College of Engineering Technology
Can Tho University
Can Tho City, Vietnam

Yu-Ming Wang
Department of Physics
National Cheng Kung University
Tainan, Taiwan

Jhao-Ying Wu
Center of General Studies
National Kaohsiung University of Science and Technology
Kaohsiung, Taiwan

1 Introduction

Tran Thi Thu Hanh, Jhao-Ying Wu,
Vo Khuong Dien, Thi Dieu Hien Nguyen,
Thi My Duyen Huynh, and Ming-Fa Lin

A lot of emergent materials, which have been/will be successfully generated by various physical and chemical methods, are outstanding candidates in exploring diverse phenomena of quasiparticle properties both theoretically and experimentally. Such unusual materials cover graphene-related systems (diamond, bulk graphites, layered graphene, carbon nanotubes, graphene nanoribbons, fullerenes, onions, and chains) [1–8], few-layer group-IV and group-V ones (silicene/germanene/tinene/plumbene/phosphorene/bismuthene/antimonene [9–15]), core anodes, electrolytes, and cathodes of lithium-ion-based batteries [e.g., the ternary lithium titanium/silicon/iron compounds [16–19]], perovskite solar cells [20], transition-/rare-earth-metal disulfide-related compounds [21, 22], and quantum topological insulators [23]. Furthermore, they are easily modulated by chemical adsorptions/substitutions [24, 25], temperatures [26], mechanical strains [27], gate voltages [electric fields] [28], uniform/non-uniform magnetic fields [29, 30], time-dependent/static Coulomb fields [31, 32], and electromagnetic waves [33]. The intrinsic and extrinsic mechanism are very sufficient for creating diversified quasiparticle behaviors. This is clearly illustrated in crystal symmetries (Moiré superlattices or not [34, 35]), electronic energy spectra and wave functions, spatial charge densities [36], van Hove singularities [37], net magnetic moments [38], and atom- and orbital-induced spin configurations [39]. Both theoretical calculations and experimental measurements are developed to examine and verify various essential properties, being attributed to the dynamic and/or static responses of the same/composite quasiparticles (e.g., electrons/polarons [40]). This book is focused on the former, which is based on first-principles simulations [41]. The critical mechanisms in determining rich and unique phenomena are thoroughly explored from consistent physical quantities, especially for the orbital hybridizations of chemical bonds and the atom- and orbital-induced magnetic configurations [42]. Most importantly, the framework of quasiparticle viewpoints could be achieved through the systematic investigations. The predicted results are compared with the measured ones in detail [43].

In general, there are two approaches of quasiparticle viewpoints in dominating the theoretical developments (all the details in Chapter 2), namely, first-principles simulations (e.g., proposed orbital hybridizations and spin configurations in Ref [43]) and the phenomenological models (e.g., the generalized tight-binding model, the modified random-phase approximation and self-energy method; [44–46]). Each strategy must have plenty of merits and drawbacks. For example, the former/the latter can/cannot successfully deal with optimal geometries, complicated band structures of

DOI: 10.1201/9781003322573-1

Moiré superlattices [34], spatial multi-orbital hybridizations [47], spin density distributions [48], the net magnetic and electric moments [49], complex excitonic effects [50], the low-dimensional quantum transports [51], and the collective atom vibrations (phonon spectra and polarization displacements [52]), while they are unable/able to explore the various magnetic quantization phenomena (e.g., the featured Landau levels/magneto-optical selection rules/magneto-electronic Coulomb excitations/quantum Hall effects [53–56]), the static/dynamic charge screening abilities (such as, the unusual Friedel oscillations due to charged impurities, plasma waves arising from the external ion beam, and the quasiparticle lifetimes of few-layer graphene/coaxial carbon nanotubes [57–59]). These have been clearly identified in systematic studies, as done for graphene-related emergent materials [60]. Apparently, how to promote their direct combinations would be very useful in understanding the same/composite quasiparticles and thus would achieve much progress of basic sciences. In this work, the VASP calculations are chosen for a theoretical development, being partially supported by the model discussions. The concise motivations of each book chapter are stated in the following paragraphs.

The various high-precision experiments are developed to detect the unusual physical/chemical/materials properties in emergent materials [the details are in Chapter 3], covering the delicate examinations and analyses about the geometric, electronic, magnetic, optical, Coulomb-excitation, and transport properties. The X-ray diffraction is frequently utilized to measure the crystal structures of bulk materials since the first theory and experiment by Bragg et al., such as the different Moiré super lattices in ternary lithium-titanium [61], lithium-silicon [62] and lithium-iron [63] oxide compounds (anode/electrolyte/cathode materials of lithium-ion-based batteries [64–66]), and stage-n graphite intercalation compounds (n corresponding to the number of graphitic layers between two intercalant ones;[67]). How to evaluate the reliable charge densities from the measured patterns are very interesting challenges. Specifically, the elastic scattering of the incident electron beams is available in observing the three-zero dimensional condensed-matter systems, in which both reflection low-energy electron diffraction (RLEED [68]) and tunneling electron microscopy (TEM [69]) are capable of providing the top and side views of surface-related structures, respectively. These two methods have clearly verified the low-dimensional crystal symmetries within the coaxial, few-layer, and deformed composite structures, such as single-/multi-walled carbon nanotubes [70], layered graphene systems with the different layers [71], normal stacking configurations [72] and twisted angles [73], planar/folded/curved/scrolled graphene nanoribbons [74–77], and buckled monolayer/bilayer silicene/germanene/tinene/plumbene [the significant coupling effects of stacking and buckling [78–81]]. As to the nano-scaled crystal structures, scanning tunneling microscopy (STM [82]) can reveal the periodical atom arrangements [83] and the local defects (vacancy, adatom intercalation and guest-atom substitution [84–86]). It is well known that STM is very successful in identifying the chirality and radius of a single-walled carbon nanotube [87], the edge boundary of an achiral/chiral graphene nanoribbon [88], the honeycomb lattices of monolayer group-IV systems [89], and the non-hexagonal phosphorene [90]. In addition, the spin-polarized STM is enhanced for its spatial resolution and thus is very useful in identifying the prominent ferromagnetism related to the atomic spin configurations [48].

The theoretical predictions on electronic energy spectra and wave functions are directly verified from scanning tunneling spectroscopy (STS [91]) and angle resolved photoemission spectroscopy (ARPES [92]). STS measurements can fully examine the dimension-dependent van Hove singularities due to the band-edge states. The very successful cases cover the geometry-determined symmetric peaks and the metallic or semiconducting behaviors in single-walled carbon nanotubes, the chirality- and width-dependent energy gaps of 1D graphene nanoribbons, the layer-number-, stacking-, twist-angle-, and doping-enriched band overlaps, band gaps, energy dispersion relations in few-layer graphene systems, and the greatly modified band properties across the Fermi level from 2D group-IV and group-V systems on distinct substrates [93]. Specifically, the spin-polarized STS measurements can distinguish the spin-split density of states [94]. On the ARPES side, their measurements can clearly reveal the quasiparticle energy spectra and lifetimes of occupied electronic states. The up-to-now works show that they have shown the diverse band dispersion for 2D materials, e.g., the linear, parabolic, partially flat, and oscillatory energy bands in AB- and ABC-stacked graphene systems [95]. The 1D graphene nanoribbons are observed to exhibit the parabolic bands in the presence of semiconducting behaviors [96]. In addition, no published papers are found about the ARPES spectra of 1D carbon nanotubes and 3D lithium titanium/silicon/iron oxides. The difficulty in defining vectors/transferred momenta and too many valence subbands should be the critical factors. Specifically, the wave-vector-dependent distribution width of ARPES spectra are available in determining the quasiparticle lifetimes, e.g., the enhanced Coulomb decay rates in monolayer alkali-doped graphene [97].

Four kinds of optical spectroscopies are able to measure the frequency-dependent reflectance [98], absorption [99], transmission [100], and photoluminescence spectra [101]. Specifically, the last ones are designed for the clear identifications of many-body effects (the greatly reduced threshold frequency, the extra-prominent absorption peaks of excitonic bound states, and the strongly modified features of single-particle vertical transitions [102]). Which kinds of measurements are suitable strongly depends on the sample thickness. For example, reflectance, transmission, and absorption spectra have been successfully measured for AB-stacked graphite [103], few-layered graphene systems with the different stacking configurations and carbon nanotubes, respectively. Furthermore, these examinations are able to clarify the low-energy π-electronic excitations and middle-energy σ-electronic ones [104], the layer-number- and stacking-enriched absorption structures [105], and the excitonic/Aharnov-Bohm effects [106]. It should be noted that the optical reflectance and photoluminescence spectra are detected for the multi-component lithium oxides [107], in which the measured results are too rough to achieve important conclusions. This is attributed to Moiré superlattices in creating a lot of valence and conduction subbands. However, the VASP simulations in this book will clearly specify the close relations between the active orbital hybridizations and the prominent absorption structures [108]. While the dynamic cases are recovered to the static ones [109] (the long wavelength limit is extended to any moment transfers [110]), the measured transport properties can clarify the semiconducting or metallic behaviors (the electron energy loss spectra are able to comprehend the single-particle and collective charge excitations [111]), especially for the quantum Hall conductivities of layered

material [56] (the unusual plasmon modes in low-dimensional systems [112]). Very interestingly, experimental measurements are frequently utilized to fully explore the screening abilities of quasiparticle charges [113].

Numerous 2D materials have been synthesized and predicted since the discovery of graphene [114]. As a result, many studies for the structures and properties of 2D materials are available [115–117]. Hexagons are basic building blocks of the crystal structures for most 2D materials. Following the structure–property relationships that have been commonly explored to discover new materials [118], we expect that the properties of 2D materials can be modified if the building blocks for these nanomaterials are changed from hexagons to pentagons. Very recently, significant efforts have focused on stabilization of the pentagonal structure based on carbons, that is monolayer penta-graphene [119]. Penta-graphene (PG) is extracted from bulk T12-carbon phase. This phase is obtained by heating an interlocking-hexagon-based metastable carbon phase at high temperature [120]. It is found that the monolayer PG is an indirect band-gap semiconductor with a band gap of ~3.25 eV [121] which is smaller than SiC [122], BN [123], and BeO [124] nanostructures. Those studies showed that this structure has obtained dynamical, thermal, and mechanical stability. In a similar way to graphene, the PG sheets can be cut along typical crystallographic orientations in order to construct various penta-graphene nanoribbons (PGNRs) to obtain quasi-one-dimensional materials. Their electronic properties were systemically investigated [125] including confinement effects and quasiparticle phenomena. The resulting four typical nanoribbons, with different edge configurations, are denoted as zigzag-zigzag penta-graphene nanoribbon (ZZ-PGNR), zigzag-armchair penta-graphene nanoribbon (ZA-PGNR), zigzag-armchair penta-graphene nanoribbon (AA-PGNR), and sawtooth-sawtooth penta-graphene nanoribbon (SS-PGNR). This study confirmed that SS-PGNR is the most stable structure when compared with the other three types of PGNRs with similar width. SS-PGNR possesses semiconductor properties. Electronic and transport properties of the sawtooth-sawtooth penta-graphene nanoribbons were systematically investigated by using the density-functional theory (DFT) in combination with the non-equilibrium Green's function (NEGF) formalism in this chapter. Quasiparticle related electronic diversity of many SS-PGNR structures is investigated in Chapter 4. This is a very important basis to find the way to realize electronic devices based on this emergent material.

A new era of low-dimensional materials has indeed opened since a two-dimensional (2D) monolayer of layered graphite was successfully isolated by Geim and Novoselov through the mechanical exfoliation method in 2004 [114, 126, 127]. This first 2D monolayer graphitic system is widely known as graphene. Graphene is made of sp^2 hybridized carbon atoms packed in a highly symmetric hexagonal lattice [128]. The honeycomb network of graphene can be extended to create the basic building block of other carbon allotropes, in which it can be stacked to form 3D graphite [129], rolled to form (1D) nanotubes [130], cut to form 1D nanoribbons [131], and wrapped to form 0D fullerenes [132]. The orbital hybridization mechanism in graphene is that the C-(2s, $2p_x$, and $2p_y$) orbitals are hybridized to create strong σ bonds to hold the planar 2D sheet, while C-$2p_z$ orbitals remain freestanding to form weak π bonding along the z-direction. This evidences that σ and π bonds in graphene are separated, in which the π orbitals mainly contribute to a Dirac cone structure at low-lying energy

[133]. Specifically, the long-range π conjugation in graphene leads to many novel quasiparticle properties that have been interested in many recent studies [134]. To date, graphene has been utilized in various applications such as flexible devices [135], transparent conductors [136], high-speed devices, and batteries [137]. Unfortunately, graphene displays many disadvantages for nanoelectronic applications due to its zero-gap feature [138]. To overcome the critical drawbacks of graphene, various approaches have been used to open a band gap in graphene, including chemical functionalizations [139], atom dopings [140], mechanical strains [141], bilayer structures [142], finite-size confinements [143], inducing defects [144], and applying external fields [145]. Beyond graphene, many efforts have been strongly focused on graphene-like 2D materials and other emergent 2D systems, including silicene [146], germanene [147], stanine [148], phosphorene [149], antimonene [150], bismuthine [151], transition metal dichalcogenides (TMDs) [152], topological insulators (TIs) [153], metal-organic frameworks (MOFs) [154], and Mxenes [155], in which silicene, a 2D analog of graphene, is made of silicon atoms packed in a low buckled honeycomb lattice. Silicene possesses many graphene-like quasiparticle features [156]; however, silicene presents better compatibility in silicon-based electronic devices than graphene so that silicene has stirred studies to extend its potential for practical applications [157]. Unlike graphene, silicene can only be synthesized through bottom-up methods due to a lack of graphite-like layered silicon structure. The most common method to synthesize the monolayer silicene is to deposit silicon atoms on the metallic substrates [158–160] that provide the experimental evidence for the presence of the 2D silicon sheet, which was theoretically predicted in 1994 [161]. Up to now, silicene has been extended in many applications, including room-temperature field-effect transistors (FETs) [162], gas sensors [163], and batteries [164]. Nevertheless, the critical disadvantage of silicene for electronic devices is its small gap feature [165]. Thus, a lot of studies have been conducted in opening band gap for silicene, including chemical modifications [166], quantum confinements [167], stacking configurations [43], mechanical strains [168], and applying external fields [169]. Among these methods, creating the finite size-quantum confinements is the most powerful way to create a band gap that can remain the low-buckled honeycomb lattice of 2D host silicene without any modification in the chemical hybridization mechanism in the honeycomb networks. The finite size confinements of 2D silicene result in 1D silicene nanoribbons (SiNRs) with armchair (ASiNR) and zigzag (ZSiNR) edges [170]. SiNRs show the middle-gap quasiparticle properties that can fully overcome the main obstacle of 2D host silicene for electronic devices [171]. On the experimental side, SiNRs have been successfully synthesized from both top-down and bottom-up methods. The top-down method is to cut the 2D host silicene to create 1D SiNRs [172], while the bottom-up approach is to grow 1D SiNRs on metallic substrates or an insulating thin film [173, 174]. SiNRs with their dominant quasiparticle features and their compatibility in silicon-based electronic devices have attracted much attention from the scientific community recently [175]. On the other hand, a wide range of applications requires materials having greater diverse quasiparticle properties such that enriching the essential quasiparticle properties of SiNRs is an interesting issue for many studies. To diversify the essential quasiparticle properties of SiNRs, various methods have been applied, including chemical dopings [176], edge passivations

[177], stacking configurations [178], generating lattice defects [179], applying external fields [180], and forming heterostructures [181], in which atom doping is the most effective way to dramatically diversify the essential quasiparticle properties. Up to now, many kinds of atoms have been successfully doped in SiNRs to result in their diversified quasiparticle properties [182–186]. However, halogen adsorptions on SiNRs have not yet been revealed in detail, while halogen adatoms with very strong electron affinity can create a strong bonding with silicon atoms to greatly complicate in chemical hybridization mechanism that can result in significant diversified quasiparticle properties. Therefore, the diverse quasiparticle properties of halogen-adsorbed SiNRs are worthy of further investigation in Chapter 5. Furthermore, the developed first-principles theoretical framework in this chapter can be fully generalized to many other emergent layered materials.

Graphene nanoribbon (GNR), a one-dimensional (1D) narrow strip of graphene [187–189], has recently attracted much attention due to its remarkable properties. 1D quantum confinement effects of a GNR can greatly diversify the essential properties, which can overcome the limitation of application in 2D graphene with its zero-gap electronic structure. Nanoribbon width and edge structure play critical roles in the essential properties of GNRs. According to the edge structure, there are two typical GNRs, armchair and zigzag ones (AGNRs and ZGNRs) [190, 191]. The former belongs to non-magnetic semiconductors, while the latter are anti-ferromagnetic middle-gap semiconductors. Up to now, GNRs have been successfully synthesized by various experimental methods such as lithographic [192, 193], sonochemical breaking [194], oxidization reaction [195], chemical vapor deposition [196], unzipping CNTs using plasma etching [197], and so on. Recently, GNRs are promising in the fields of energy storages, e.g., field-effect transistors [198], lithium-ion batteries [199, 200], and fuel cells [201]. To further expand the range of application, GNRs' properties can be modulated by changing the geometric structures [202, 203], doping [204, 205], and applying external electric/magnetic fields [206, 207]. Chapter 6 aims to provide a systematic study on the fundamental properties of the metal/transition metal adatom-adsorbed GNRs. The various Al-/Fe-/Co-/Ni-adsorption structures, critical multi-orbital hybridizations, significant non-magnetism (NM)/anti-ferromagnetism (AFM)/ferromagnetism (FM), and metallic/semiconducting behaviors will be clearly illustrated.

A single-wall carbon nanotube as well as silicon nanotube can be regarded as a rolled honeycomb lattice of graphene and silicene, respectively. The successful systematic studies of carbon nanotubes (CNTs) have been synthesized by means of arc-discharge evaporation in 1991 [208]. Later, other developments [209–213] such as characterization [214–217], property [218–220], and applications [221–223] sprang up like mushrooms. Similarly, silicon nanotubes (SiNTs) were successful initially synthesized in 2000 via ozone to remove the tubular meso- and nanoporous silicate templates [223]. Soon after that, a lot of investigations have been reported such as different growth process [224–226], features [226, 227], and applications [228–230]. The electronic properties of the planar graphene nanoribbons exhibit semiconducting behavior. On the other hand, the cylindrical carbon nanotubes are metals or direct-gap semiconductors sensitive to the chirality and radius. Metallic nanotubes are exclusively comprised of either armchair nanotubes or very small zigzag nanotubes

with radii < $\sqrt{3}b$ (b is the C-C bond length) [231]. The cylindrical silicon nanotubes exhibit the same behaviors as carbon nanotubes. They can be either metallic or semiconducting depending on the radii and chiral vectors. The Metallic silicon nanotubes are only comprised of zigzag types, especially for the small size of tubes ((m,0), m ≦9), and others are semiconducting such as armchair silicon nanotubes and large size of zigzag ones. Large curvature effect enhances the σ and π mixing in the smaller tubes, leading to the metallic property. The theoretical calculations [232, 233] and experimental measurement have confirmed the curvature effects, the misorientations of $2p_z$ orbitals and hybridizations of carbon (2s, $2p_x$, $2p_y$, $2p_z$) and silicon (3s, $3p_x$, $3p_y$, $3p_z$) four orbitals, on a cylindrical surface, leading to the geometry dependent energy gaps. Chapter 7 introduces single-wall carbon and silicon nanotubes with different diameters and chiralities. The geometric structure, energy bands, spatial charge distributions, and orbital-projected density of states are discussed in detail. Silicon nanotube is characterized by sp^3 hybridization and the gear-like structure. The ground state energy E_0 obviously decreases with the increasing diameter, owing to the reduction of bond length, buckling distance (for SiNTs), and curvature effect. The variation of the band structure and PDOSs with the curvature is investigated thoroughly. The calculated results clearly indicate the unusual features of the energy band, such as energy gap, energy dispersions, band-edge states, mixing bands, band overlap, and state degeneracy. The total and local DOSs exhibit a plenty of prominent asymmetric peaks in the inverse of the square-root form. The zigzag carbon and silicon nanotubes are quite different from each other, mainly owing to the curvature effect, unsymmetrical structure, and the open/periodical boundary condition. These could be directly verified by the STS measurements.

Chapter 8 offers an analysis of electronic, optical properties of pristine silicene and substituted-silicene by B, C, and N atoms using density functional theory. Such guest-atoms possess three, four, and five electrons in the outermost cell, being suitable for a deep understanding of the quasiparticle properties of the substitutional silicene systems. The optical coefficients such as the real and imaginary dielectric function, dielectric function, electron loss function, absorption coefficient, refractivity, and reflectivity are calculated for both in-plane light polarization (perpendicular) and out of plane (parallel) polarization. The electronic and optical properties of the guest-substituted silicene systems become so different compare with the pristine ones. Our computational results present the p-type doping metallic behavior in boron-substituted silicene while in the carbon- and nitrogen-substituted cases, the systems become semiconductoring phenomena. The absorption intensity in the case of carbon-substituted silicene is highest in both polarization directions, but in the case of boron and nitrogen, it is almost unchanged compared to pristine. The comparison between the guest-atoms substitution and the pristine systems will be discussed in detail in all the properties.

Binary compounds, fully B-/C-/N-substituted germanenes, exhibit the diversified phenomena through the different chemical bondings presented in Chapter 9. The delicate first-principles calculations can present the buckling/planar honeycomb lattices, the atom-dominated band structures, the spatial charge densities, the spin density distributions, and the atom-, orbital-, and spin-decomposed density of states, being very useful in determining the critical orbital hybridizations and magnetic

configurations. The concise pictures, the strong competition between sp^2 and sp^3 bondings, and the guest-dependent spin states, are responsible for the geometric symmetries, the metallic/wide-/narrow-gap behaviors, the modification/destruction of Dirac-cone structures, the nonmagnetic or ferromagnetic properties, the crossings/anti-crossings of π and σ bands, or the pure sp^3 energy bands.

Plumbene, the latest cousin of graphene, has been mentioned as a candidate material for topological insulator (TI) and room-temperature operations [12, 234] due to its rich and unique geometric and electronic properties. In 2019, Yuhara and his coworkers reported the successful fabrication of the single layer of lead atoms by molecular beam epitaxy (MBE) [235]. This work has prompted the development of related research, e.g., chemical decoration and/or hydrogenate of monolayer Plumbene. The chemical modifications, as revealed in the experimental and theoretical investigations [236, 237], are one of the most efficient approaches in dramatically changing the geometric, electronic, and optical properties through orbital hybridization modification. Very interestingly, the Hydrogen atom with 1s orbital in the electronic configuration exhibits the extremely strong chemical bonding with the Pb atom in Plumbene. The critical quasiparticle features include the significant orbital hybridizations in Pb-H chemical bonds, the significant change of the electronic properties in double and single side adsorption, the modify of optical spectrum in case of with/without excitonic effect, and very importantly, the effect of spin-orbital couplings on the electronic and optical properties of the hydrogenated systems are thoroughly examined from the first-principles simulations in Chapter 10. The current study is very useful in comprehending the crucial properties of 2D materials with chemical functionality.

Graphite is one of the mainstream materials in basic science research and potential applications [238]. Apparently, this system stirred plenty of theoretical and experimental [239, 240] studies more than one hundred years ago. Its layered structure, which consists of carbon mb lattices, exhibits the unusual crystal symmetries [241] and thus the unusual phenomena, such as, the AA [242], AB [242], ABC [243], and turbostratic stackings [244]. The graphitic spacing, being determined by the Van der Waals interactions [245], provides a very active environment in creating the chemical intercalations or de-intercalations for the various atoms/molecules/ions [246], especially for the charging and discharging processes in ion-based batteries [247]. The chemical modifications are capable of generating the n-, p-type dopings [248] or even the zero-gap semiconducting behaviors [249], the drastic changes of band structures and van Hove singularities through the zone-folding effects and significant intercalant-related interactions [13], the featured optical reflectance and absorption spectra in the presence/absence of quasi-stable excitons [250], the diverse (momentum, frequency)-dependent Coulomb excitations under distinct free carriers (the rich electron-hole and collective excitations), the very high electrical conductivities comparable to those metals, and a great enhancement of the superconducting transition temperature [250]. Very interestingly, this rather stable system is frequently utilized as the anode/cathode materials of lithium/aluminum-based batteries. The rich essential properties have been studied for the Li- and Li^+-related graphite intercalation compounds [249]. The critical quasiparticle properties, the significant orbital hybridizations in various intralayer and interlayer chemical bonds, are thoroughly

examined from the first-principles simulations in Chapter 11. The intercalations and de-intercalations of large molecules are expected to become more complicated, mainly owing to the enlarged Moiré superlattices [251]. This study is very useful in comprehending aluminum-based batteries [252], certain important differences among the different graphite intercalation compounds, and close relations between the numerical methods and the phenomenological models [253].

Batteries [254], which store and release energy in terms of chemical energy, have become one of the mainstream items in research recently. Compared with other energy store systems, lithium-ion-based batteries (LIBs) have received a great deal of attention since they process desirable features, such as light weight, long life cycle, fast charging time, and ability to provide a sizable electronic current for electronic devices [255, 256]. Generally speaking, the commercial LIB is a complex combination of the electrolyte with the negative (cathode) and the positive (anode) electrodes [255, 256]. Furthermore, the physical/chemical pictures in each component are rather complicated and directly related to the performance of storage systems. The previous few theoretical studies are conducted on the geometric and electronic properties of LIBs' components through the first-principles calculations. However, the delicate results and analyses have been thoroughly absent up to now. That is to say, the calculated results are insufficient, and there are no critical mechanisms (concise physical pictures) in comprehending the diversified phenomena. The theoretical framework is based on the numerical calculations and delicate analyses were developed and applied for the layered $LiFeO_2$-a candidate for cathode compound in Chapter 12. The fundamental features, the critical quasiparticle properties, and the significant orbital hybridizations in various chemical bonds are thoroughly examined from the first-principles simulations. The charging and discharging of LIBs are expected to be complicated owing to the variation of chemical bonds and thus, orbital hybridizations. Our predictions provide certain meaningful information about the critical physical/chemical pictures in LIBs. Such state-of-the-art analysis is very useful for fully comprehending the diversified properties in anode/cathode/electrolyte and other emerging materials.

Beyond graphene, atomically thin TMDs have become a new flatform owing to their rich and unique properties [257–260]. Especially, the change in properties from monolayer to bilayer is more significant than that resulting from multilayers [261–264]. Bilayer TMDs reveal the interesting and unique properties compared to their monolayers such as higher density of states and carrier mobility [265–268]. This phenomenon anticipates superior performance in thin-film transistors and sensors. In addition, stacking orders in bilayer exhibit an alternative method in investigating their effects. Varying stacking modes in structural engineering can manipulate the electronic properties of bilayer TMDs as reported in MoS_2 [269–271] and WS_2 [272]. Among TMDs, HfX_2 (X = S, Se, or Te) is a group candidate that promises opportunities for investigation and applications based on their emergent and satisfactory findings. In the attempt to vary layered materials for reduction in the size of devices, layered structures such as monolayer or bilayer have been concerned. Besides, bulk and monolayer of HfX_2 had been explored and used in some electronic devices [273–276]. Bilayer HfX_2 should be therefore analyzed in order to enhance this group. Although bilayer $HfSe_2$ [277] has been studied and found promising for

thermal conductivity, the perspective of all these materials in bilayer is still limited. Using VASP calculations, the quasiparticle problems related to electrons as formerly mentioned are resolved, indicating the close relations between theoretical framework and quasiparticles. In Chapter 13, we focus on the electronic properties of these materials constructed in bilayer to provide further information about their features.

Lithium-ion batteries have become popular and dominate in commercial purposes. They possess many high-performance characteristics such as high power, energy density, long life cycle, and friendly to the environment, as well as affordable prices. Many candidates are investigated further as potential cathode, anode, and electrolyte components. Our study in this chapter focuses on an excellent anode material with the zero-strain property of the volume during the lithium intercalation or deintercalation process. The ternary compound possesses a lot of advantages, e.g., the safety and long cycling life for lithium-ion batteries. Currently, $Li_4Ti_5O_{12}$ enters into the commercial anode product for Li^+-ion based batteries [278, 279]. Lithium titanate material presents rich and unique geometric, electronic properties under the quasiparticle framework [39, 278, 279]. The primitive cell contains a huge number of atoms, which is called a Moiré superlattice [39]. The geometric structure performs a non-uniform environment, which fundamentally comes from the Li-O and Ti-O bonds. Many significant electronic quasiparticle properties are presented such as band structures, atom-dominated energy spectrum, spatial charge density distributions, and the atom- or the orbital-decomposed density of states [279]. The theoretical quasiparticle properties could be tested under the high-resolution experimental measurements. Many experimental examinations can be used for investigating the whole structures, e.g., X-ray diffractions for measuring the lattice parameters, transmission electron microscopy (TEM) for morphology [280], angle-resolved photoemission spectroscopy (ARPES [281–283]), and scanning tunneling spectroscopy (STS [283–285]) for band structures examination along with van Hove singularities. Also, the theoretical development of a quasiparticle framework in geometry and the electronic in terms of multi-hybridizations is worthy to thoroughly investigate in Chapter 14.

In Chapter 15, the theoretical calculations for the low-lying vibrational H atoms adsorbed on the Pt(110) surface are presented. We use the H/Pt(110) model with the conventional ultrahigh vacuum (UHV) and the density functional theory (DFT) to study the phonon frequency (the quasiparticle frequency). The nature of hydrogen atoms, which were adsorbed on the four different sites of the Pt(110) surface, is shown. The most stable site of the short bridge is in agreement with previous studies. The highest stretching frequency of 2200 cm^{-1} and the zero-point energy (ZPE) of the H atom on the top site ~140 meV are calculated. Our results convincingly demonstrate the need to study the local oscillation to understand the dynamics of this system.

Bismuth chalcogenides are of great interest because of the exciting properties of topological insulators (TIs) and their potential applications in low power dissipation electronic devices, spintronics, and quantum computing. TIs are exotic materials with an insulating bulk and topologically protected surface states (TSSs) that exhibits Dirac linear energy dispersion inside the bulk gap, spin-polarization by spin-momentum locking nature. In bismuth chalcogenide TIs (e.g., Bi_2Te_3, Bi_2Se_3,

Bi_2Se_2Te, etc.), the dominant bulk conduction arising from naturally occurring crystal imperfections and residual carrier doping has greatly hindered the detection of Dirac fermions by means of weak anti-localization effect (WAL) and quantum oscillations at low temperatures. Regardless of such challenges, the transport method has been great success in probing the TSSs and studying its properties. The WAL effect agrees well with the Hikami-Larkin-Nagaoka model that allows to obtain the number of conduction channel and phase coherent length. However, in TIs, since the WAL reflects both the 3D contribution of spin–orbit coupling in bulk and the Dirac nature of the 2D TSSs, a detailed study of magnetoconductance (ΔG (θ, B)) in tilted magnetic fields (θ = 0–90°) is essential to get insight into the origin of the observed WAL. If all the ΔG curves coincide with each other in the plot of ΔG (θ, B) versus the perpendicular component of the magnetic field, then the observed WAL effect is 2D in nature. In addition, TIs with sufficiently high surface electron mobility can present pronounced Shubnikov–de Haas (SdH) oscillations. The analysis of SdH oscillations leads to elucidating the Dirac nature of TSS with finite Berry phase and 2D Fermi surface; it also enables us to extract the carrier concentration, effective mass, Dingle temperature, and the Berry phase of TIs. Chapter 16 presents the recent advances in magnetotransport method to study on bismuth chalcogenide TIs and their most fascinating results.

Current emerging materials provide us with various significant applications in industry, particularly in energy storage and electronic equipment. In battery applications, $LiFeO_2$ can be served as a cathode material, while silicon-carbon nanotubes and $Li_4Ti_5O_{12}$ are popular for the anode side. Aluminum-chloride-graphene intercalated compounds are known as an abundant and friendly environment, which can contribute to the development of ion-based batteries. Other materials have significant applications in electronic and photoelectronic devices such as transition metal dichalcogenides (TMDs) material group HfX_2 (X = S, Se, or Te), Bismuth chalcogenide topological insulators (BiCh-TIs). In addition, penta-graphene nanoribbons metals/transition metals and halogen-adsorbed silicene nanoribbons can be developed for certain heterojunction devices and spintronics, respectively. Remarkably, spintronics is used to monitor the spin properties, which are based on the natural characteristics of electrons. Furthermore, hydrogenated absorption systems, for example, the adsorbed hydrogen on the Pt(110) surface, plumbene adsorption hydrogen, and hydrogen adsorption on two-dimensional germanene are developed to enhance hydrogen technology and battery applications. substituted silicene systems germanene and silence systems can be useful for light and lasers due to their wide band gap. Chapter 17 will present diverse practical contributions of these materials in industrial and daily applications.

In summary, Chapter 2 covers the theoretical frameworks of quasiparticle particles from both viewpoints of first-principles simulations and phenomenological models [286], as generalized from the precious developments [287]. The high-resolution experimental measurements are thoroughly characterized in Chapter 3. By delicate VASP calculations and analyses, the diverse quasiparticle phenomena clearly reveal in penta-graphene nanographene nanoribbons [Chapter 4], halogenated silicene nanoribbons [Chapter 5], metals/transition metals-adsorbed graphene nanoribbons [Chapter 6], zigzag silicon nanotubes [Chapter 7], boron-/carbon-/

nitrogen-substituted silicene [Chapter 8], adatom-substituted on germanene systems [Chapter 9], hydrogen-chemisorption plumbenes [Chapter 10], stage-1/stage-2/stage-3/stage-4 $AlCl_4$ graphite intercalation compounds [Chapter 11], ternary lithium iron oxides [Chapter 12], different stacking in bilayer HfX_2 (X=S, Se, or Te) [Chapter 13], lithium titanium oxides [Chapter 14], H-adsorbed Pt(110) surfaces [Chapter 15], and bismuth Chalcogenide topological Insulators [Chapter 16]. In addition to the theoretical analysis, the diverse related practical applications of these emerging materials will be covered in this book [Chapter 17].

In concluding remarks, the calculated results include the total ground state energies/the chemical modification energies [288], the optimal Moiré superlattices/normal unit cells [289], the atom- and spin-dominated band structures/wave functions [25], the spatial charge/spin density distributions [36], the atom- orbital- and spin-decomposed van Hove singularities [37], the net magnetic moments [205], the single-particle and many-body reflectance [290], absorption [291], transmission [292] and energy loss spectra [293], the ballistic electrical conductivities [294], the Hall quantum ones [295], and the vibration phonons [296]. They are very sufficient in identifying the various quasiparticle behaviors and further generalize the previous theoretical framework [297]. Concluding remarks, open issues, and obvious problems are, respectively, illustrated in Chapter 18–20.

REFERENCES

[1] Erohin S V, Ruan Q Y, Sorokin P B and Yakobson B I 2020 Nano-thermodynamics of chemically induced graphene-diamond transformation *Small* **16**

[2] Lee S M, Kang D S and Roh J S 2015 Bulk graphite: materials and manufacturing process *Carbon letters* **16** 135–46

[3] Weibel A, Flaureau A, Pham A, Chevallier G, Esvan J, Estournes C and Laurent C 2020 One-step synthesis of few-layered-graphene/alumina powders for strong and tough composites with high electrical conductivity *J Eur Ceram Soc* **40** 5779–89

[4] Stefan-van Staden R I and Comnea-Stancu I R 2021 Chiral single-walled carbon nanotubes as chiral selectors in multimode enantioselective sensors *Chirality* **33** 51–8

[5] Pawlak R, Liu X S, Ninova S, D'Astolfo P, Drechsel C, Sangtarash S, Haner R, Decurtins S, Sadeghi H, Lambert C J, Aschauer U, Liu S X and Meyer E 2020 Bottom-up synthesis of Nitrogen-doped porous graphene nanoribbons *J Am Chem Soc* **142** 12568–73

[6] Artyukh A A and Chernozatonskii L A 2020 Simulation of the formation and mechanical properties of layered structures with polymerized fullerene-graphene components *Jetp Lett* **111** 109–15

[7] Liu Y Y and Kim D Y 2015 Ultraviolet and blue emitting graphene quantum dots synthesized from carbon nano-onions and their comparison for metal ion sensing *Chem Commun* **51** 4176–9

[8] Gao E L, Li R S and Baughman R H 2020 Predicted confinement-enhanced stability and extraordinary mechanical properties for carbon nanotube wrapped Chains of linear carbon *Acs Nano* **14** 17071–9

[9] An X T, Zhang Y Y, Liu J J and Li S S 2013 Quantum spin hall effect induced by electric field in silicene *Appl Phys Lett* **102**

[10] Zhao F L, Wang Y, Zhang X, Liang X J, Zhang F, Wang L, Li Y, Feng Y Y and Feng W 2020 Few-layer methyl-terminated germanene-graphene nanocomposite with high capacity for stable lithium storage *Carbon* **161** 287–98

[11] Chen R B, Chen S C, Chiu C W and Lin M F 2017 Optical properties of monolayer tinene in electric fields *Sci Rep-Uk* **7**
[12] Mahmud S and Alam M K 2019 Large band gap quantum spin Hall insulator in methyl decorated plumbene monolayer: A first-principles study *Rsc Adv* **9** 42194–203
[13] Suragtkhuu S, Bat-Erdene M, Bati A S R, Shapter J G, Davaasambuu S and Batmunkh M 2020 Few-layer black phosphorus and boron-doped graphene based heteroelectrocatalyst for enhanced hydrogen evolution *J Mater Chem A* **8** 20446–52
[14] Zhong W, Zhao Y, Zhu B B, Sha J J, Walker E S, Bank S, Chen Y F, Akinwande D and Tao L 2020 Anisotropic thermoelectric effect and field-effect devices in epitaxial bismuthene on Si (111) *Nanotechnology* **31**
[15] Zou H, Zhang H, Yang Z X and Zhang Z H 2021 Magneto-electronic and spin transport properties of transition metal doped antimonene nanoribbons *Physica E* **126**
[16] Srout M, El Kazzi M, Ben Youcef H, Fromm K M and Saadoune I 2020 Improvement of the electrochemical performance by partial chemical substitution into the lithium site of titanium phosphate-based electrode materials for lithium-ion batteries: LiNi0.25Ti1.5 Fe-0.5(PO4)(3) *J Power Sources* **461**
[17] Tang F Q, Jiang T T, Tan Y, Xu X Y and Zhou Y K 2021 Preparation and electrochemical performance of silicon@graphene aerogel composites for lithium-ion batteries *J Alloy Compd* **854**
[18] Zhu Y, He X and Mo Y 2017 Strategies based on nitride materials chemistry to stabilize Li metal anode *Adv Sci* **4**(8) 1600517
[19] Rowsell J L C, Pralong V and Nazar L F 2001 Layered lithium iron nitride: A promising anode material for li-ion batteries *J Am Chem Soc* **123** 8598–9
[20] Haque F, Yi H M, Lim J, Duan L P, Pham H D, Sonar P and Uddin A 2020 Small molecular material as an interfacial layer in hybrid inverted structure perovskite solar cells *Mat Sci Semicon Proc* **108**
[21] Dong S J, Du J T, Lu Y L, Li J S, Wang L and Zhao H 2021 Ab initio identification of two-dimensional square-octagonal bismuthene doped with 3d transition metals as potential spin gapless semiconductor, bipolar magnetic semiconductor, and quantum anomalous Hall insulator *Physica E* **126**
[22] Zhang Y, Li K D and Liao J 2020 Facile synthesis of reduced-graphene-oxide/rare-earth-metal-oxide aerogels as a highly efficient adsorbent for rhodamine-B *Appl Surf Sci* **504**
[23] Tahir M, Manchon A, Sabeeh K and Schwingenschlogl U 2013 Quantum spin/valley hall effect and topological insulator phase transitions in silicene *Appl Phys Lett* **102**
[24] Luo Y, Ito Y, Zhong H F, Endou A, Kubo M, Manogaran S, Imamura A and Miyamoto A 2004 Density functional theory and tight-binding quantum chemical molecular dynamics calculations on Ce1-xCuxO2-delta catalyst and the adsorptions of CH3OH and CH3O on Ce1-xCuxO2-delta *Chem Phys Lett* **384** 30–4
[25] Pham H D, Su W P, Nguyen T D H, Tran N T T and Lin M F 2020 Rich p-type-doping phenomena in boron-substituted silicene systems *Roy Soc Open Sci* **7**
[26] Wu J Y, Chen S C and Lin M F 2014 Temperature-dependent Coulomb excitations in silicene *New J Phys* **16**
[27] Sun J, Yuan K P, Zhou W Y, Zhang X L, Onoe J, Kawazoe Y and Wang Q 2020 Low thermal conductivity of peanut-shaped carbon nanotube and its insensitive response to uniaxial strain *Nanotechnology* **31**
[28] Dutta R, Paitya N and Subash T D 2020 Electric field and surface potential analytical modeling of novel Double Gate Triple Material PiN Tunneling Graphene Nano Ribbon FET (DG-TM-PiN-TGNFET) *Silicon-Neth*

[29] Ebrahimr F, Nouraeil M, Dabbagh A and Civalek O 2019 Buckling analysis of graphene oxide powder-reinforced nanocomposite beams subjected to non-uniform magnetic field *Struct Eng Mech* **71** 351–61
[30] de Souza J F O, Ribeiro C A D and Furtado C 2014 Bound states in disclinated graphene with Coulomb impurities in the presence of a uniform magnetic field *Phys Lett A* **378** 2317–24
[31] Sindona A, Pisarra M, Gomez C V, Riccardi P, Falcone G and Bellucci S 2017 Calibration of the fine-structure constant of graphene by time-dependent density-functional theory *Phys Rev B* **96**
[32] Despoja V, Mowbray D J, Vlahovic D and Marusic L 2012 TDDFT study of time-dependent and static screening in graphene *Phys Rev B* **86**
[33] Ma Y, Lv C, Tong Z, Zhao C F, Li Y S, Hu Y Y, Yin Y H, Liu X B and Wu Z P 2020 Single-layer copper particles integrated with a carbon nanotube film for flexible electromagnetic interference shielding *J Mater Chem C* **8** 9945–53
[34] Gao Y, Lin X Q, Smart T, Ci P H, Watanabe K, Taniguchi T, Jeanloz R, Ni J and Wu J Q 2020 Band engineering of large-twist-angle graphene/h-BN Moire superlattices with pressure *Phys Rev Lett* **125**
[35] Dean C R, Wang L, Maher P, Forsythe C, Ghahari F, Gao Y, Katoch J, Ishigami M, Moon P, Koshino M, Taniguchi T, Watanabe K, Shepard K L, Hone J and Kim P 2013 Hofstadter's butterfly and the fractal quantum Hall effect in moire superlattices *Nature* **497** 598–602
[36] Pham H D, Gumbs G, Su W P, Tran N T T and Lin M F 2020 Unusual features of nitrogen substitutions in silicene *Rsc Adv* **10** 32193–201
[37] Pham H D, Lin S Y, Gumbs G, Khanh N D and Lin M F 2020 Diverse properties of carbon-substituted silicenes *Front Phys-Lausanne* **8**
[38] Muhammad I K, Swera K and Abdul M 2021 Computational study of 4d transition metals doped bismuthene for spintronics *Physica E* **126**
[39] Nguyen T D H, Pham H D, Lin S Y and Lin M F 2020 Featured properties of Li+-based battery anode: Li4Ti5O12 *Rsc Advances* **10** 14071–9
[40] Peithmann K, Korneev N, Flaspohler M, Buse K and Kratzig E 2000 Investigation of small polarons in reduced iron-doped lithium-niobate crystals by non-steady-state photocurrent techniques *Physica Status Solidi a-Applied Research* **178** R1–R3
[41] Chepkasov I V, Ghorbani-Asl M, Popov Z I, Smet J H and Krasheninnikov A V 2020 Alkali metals inside bi-layer graphene and MoS2: Insights from first-principles calculations *Nano Energy* **75**
[42] Lin S Y, Chang S L, Tran N T T, Yang P H and Lin M F 2015 H-Si bonding-induced unusual electronic properties of silicene: A method to identify hydrogen concentration *Phys Chem Phys* **17** 26443–50
[43] Lin S Y L H Y, Nguyen D K, Tran N T T, Pham H D, Chang S L, Lin C Y and Lin M F 2020 *Silicene-Based Layered Materials* (IOP Publishing)
[44] Lee S M and Niehaus T A 2020 Simulation of structural evolution using time-dependent density-functional based tight-binding method *J Nanosci Nanotechno* **20** 7206–9
[45] Paier J, Ren X, Rinke P, Scuseria G E, Gruneis A, Kresse G and Scheffler M 2012 Assessment of correlation energies based on the random-phase approximation *New J Phys* **14**
[46] Shishkin M and Kresse G 2007 Self-consistent GW calculations for semiconductors and insulators *Phys Rev B* **75**
[47] Dien V K, Han N T, Nguyen T D H, Huynh T M D, Pham H D and Lin M F 2020 Geometric and electronic properties of Li2GeO3 *Front Mater* **7**

[48] Zhao P and Chen G 2020 Spin-polarized transport properties and spin molecular Boolean logic gates in planar four-coordinate Fe complex-based molecular devices with carbon nanotube bridges and electrodes *J Magn Magn Mater* **493**
[49] Liu P T, Franchini C, Marsman M and Kresse G 2020 Assessing model-dielectric-dependent hybrid functionals on the antiferromagnetic transition-metal monoxides MnO, FeO, CoO, and NiO *J Phys-Condens Mat* **32**
[50] Liu P T, Kim B, Chen X Q, Sarma D D, Kresse G and Franchini C 2018 Relativistic GW plus BSE study of the optical properties of Ruddlesden-Popper iridates *Phys Rev Mater* **2**
[51] Yin Y H, Shao C, Zhang C, Zhang Z F, Zhang X W, Robertson J and Guo Y Z 2020 Anisotropic transport property of antimonene MOSFETs *Acs Appl Mater Inter* **12** 22378–86
[52] Bridges A, Yacoot A, Kissinger T and Tatam R P 2020 Polarization-sensitive transfer matrix modeling for displacement measuring interferometry *Appl Optics* **59** 7694–704
[53] Garcia-Flores A F, Terashita H, Granado E and Kopelevich Y 2010 Landau levels in bulk graphite by Raman spectroscopy (vol 79, 113105, 2009) *Phys Rev B* **81**
[54] Lin C Y, Wu J Y, Chang C P and Lin M F 2014 Magneto-optical selection rules of curved graphene nanoribbons and carbon nanotubes *Carbon* **69** 151–61
[55] Fandan R, Pedros J, Guinea F, Bosca A and Calle F 2019 Effect of quasiparticle excitations and exchange-correlation in Coulomb drag in graphene *Commun Phys-Uk* **2**
[56] Bao H R, Liao W H, Zhang X C, Yang H, Yang X X and Zhao H P 2017 Photoinduced quantum spin/valley hall effect and its electrical manipulation in silicene *J Appl Phys* **121**
[57] Affleck I, Borda L and Saleur H 2008 Friedel oscillations and the Kondo screening cloud (vol 77, art no 180404, 2008) *Phys Rev B* **78**
[58] Li H Y, Utama M I B, Wang S, Zhao W Y, Zhao S H, Xiao X, Jiang Y, Jiang L L, Taniguchi T, Watanabe K, Weber-Bargioni A, Zettl A and Wang F 2020 Global control of stacking-order phase transition by doping and electric field in few-layer graphene *Nano Lett* **20** 3106–12
[59] Chan Y 2020 A continuum study of ionic layer analysis for single species ion transport in coaxial carbon nanotubes *Epl-Europhys Lett* **131**
[60] Lin C Y C R B, Ho Y H and Lin F L 2020 *Electronic and Optical Properties of Graphite Related Systems* ([S.l.]: CRC Press)
[61] Abraham K M, Holleck G L, Nguyen T, Pasquariello D M and Schwartz D A 1989 The lithium titanium disulfide secondary battery *J Power Sources* **26** 313–17
[62] Uxa D, Huger E, Dorrer L and Schmidt H 2020 Lithium-silicon compounds as electrode material for Lithium-Ion batteries *J Electrochem Soc* **167**
[63] Wang S H, Yang Y and Guo K H 2020 An improved recursive total least squares estimation of capacity for electric vehicle lithium-iron phosphate batteries *Math Probl Eng* **2020**
[64] Li M, Liu T C, Bi X X, Chen Z W, Amine K, Zhong C and Lu J 2020 Cationic and anionic redox in lithium-ion based batteries *Chem Soc Rev* **49** 1688–705
[65] Chen J M, Xiong J W, Ji S M, Huo Y P, Zhao J W and Liang L 2020 All solid polymer electrolytes for lithium batteries *Prog Chem* **32** 481–96
[66] Ramzan M, Lebegue S and Ahuja R 2009 Ab initio study of lithium and sodium iron fluorophosphate cathodes for rechargeable batteries *Appl Phys Lett* **94**
[67] Li W B, Lin S Y, Tran N T T, Lin M F and Lin K I 2020 Essential geometric and electronic properties in stage-ngraphite alkali-metal-intercalation compounds *Rsc Adv* **10** 23573–81

[68] Ahmed R, Nakagawa T and Mizuno S 2020 Structure determination of ultra-flat stanene on Cu(111) using low energy electron diffraction *Surf Sci* **691**
[69] Khramov E V, Privezentsev V V, Palagushkin A N, Shcherbachev K D and Tabachkova N Y 2020 XAFS and TEM investigation of nanocluster formation in (64)Zn(+) ion-implanted and thermo-oxidized SiO(2) film *J Electron Mater* **49** 7343–8
[70] Kamedulski P, Zielinski W, Nowak P, Lukaszewicz J P and Ilnicka A 2020 3D hierarchical porous hybrid nanostructure of carbon nanotubes and N-doped activated carbon *Sci Rep-Uk* **10**
[71] Chittari B L, Chen G R, Zhang Y B, Wang F and Jung J 2019 Gate-tunable topological flat bands in trilayer graphene boron-nitride moire superlattices *Phys Rev Lett* **122**
[72] Ho Y H, Chiu Y H, Lin D H, Chang C P and Lin M F 2010 Magneto-optical selection rules in Bilayer Bernal Graphene *Acs Nano* **4** 1465–72
[73] Wang J, Bo W, Ding Y, Wang X and Mu X 2020 Optical, optoelectronic, and photoelectric properties in moire superlattices of twist bilayer graphene *Mater Today Phys* **14**
[74] Talantsev E F, Mataira R C and Crump W P 2020 Classifying superconductivity in moire graphene superlattices *Sci Rep-Uk* **10**
[75] He Y, Xiang K X, Zhou W, Zhu Y R, Chen X H and Chen H 2018 Folded-hand silicon/carbon three-dimensional networks as a binder-free advanced anode for high-performance lithium-ion batteries *Chem Eng J* **353** 666–78
[76] Slepchenkov M M and Glukhova O E 2020 Improving the sensory properties of layered phospholipid-graphene films due to the curvature of graphene layers *Polymers-Basel* **12**
[77] Sidorov A, Mudd D, Sumanasekera G, Ouseph P J, Jayanthi C S and Wu S Y 2009 Electrostatic deposition of graphene in a gaseous environment: A deterministic route for synthesizing rolled graphenes? *Nanotechnology* **20**
[78] Shih P H, Do T N, Gumbs G, Pham H D and Lin M F 2019 Electric-field-diversified optical properties of bilayer silicene *Opt Lett* **44** 4721–4
[79] Pham H D, Nguyen T D H, Vo K D, Huynh T M D and Lin M F 2020 Rich essential properties of boron, carbon, and nitrogen substituted germanenes *Appl Phys Express* **13**
[80] Matthes L, Pulci O and Bechstedt F 2014 Optical properties of two-dimensional honeycomb crystals graphene, silicene, germanene, and tinene from first principles *New J Phys* **16**
[81] Yuhara J and Le Lay G 2020 Beyond silicene: Synthesis of germanene, stanene and plumbene *Jpn J Appl Phys* **59**
[82] Bezerra L G P, Souza A L P, Lago A E A, Campos L B, Nunes T L, Paula V V, Oliveira M F and Silva A R 2019 Addition of equex STM to extender improves post-thawing longevity of collared peccaries' sperm *Biopreserv Biobank* **17** 143–7
[83] Song S K, Kim T H and Yeom H W 2019 Atomic structures of self-assembled epitaxially grown GdSi2 nanowires on Si(001) by STM *Sci Rep-Uk* **9**
[84] Hu Y H, Shu T, Mao C X, Xue L, Yan Z and Wu Y Y 2019 Arsenene and antimonene doped by group-VA atoms: First-principles studies of the geometric structures, electronic properties and STM images *Physica B* **553** 195–201
[85] Wang H X, Wu C H, Eren B, Hao Y B, Feng B M, Fang H T and Salmeron M 2019 Operando STM study of the interaction of imidazolium-based ionic liquid with graphite *Energy Storage Mater* **20** 139–45
[86] Haga T, Fujimoto Y and Saito S 2019 STM visualization of carbon impurities in sandwich structures consisting of hexagonal boron nitride and graphene *Jpn J Appl Phys* **58**
[87] Hong L, Gao D M, Wang J R and Zheng D 2020 Adsorption simulation of open-ended single-walled carbon nanotubes for various gases *Aip Adv* **10**
[88] Gao J, Uribe-Romo F J, Saathoff J D, Arslan H, Crick C R, Hein S J, Itin B, Clancy P, Dichtel W R and Loo Y L 2016 Ambipolar transport in solution-synthesized graphene nanoribbons *Acs Nano* **10** 4847–56

[89] Grzybowski G, Ware M E, Kiefer A and Claflin B 2020 Design of a remote plasma-enhanced chemical vapor deposition system for growth of tin containing group-IV alloys *J Vac Sci Technol B* **38**
[90] Arcudia J, Kempt R, Cifuentes-Quintal M E, Heine T and Merino G 2020 Blue phosphorene bilayer is a two-dimensional metal and an unambiguous classification scheme for buckled hexagonal bilayers *Phys Rev Lett* **125**
[91] Liu R Z, Ye Z Y, Wang J H and Liu L M 2019 Lifthitz transition and shadow gap in Li(Fe1-xCox) as investigated by STM/STS *J Supercond Nov Magn* **32** 3789–95
[92] Iwasawa H, Dudin P, Inui K, Masui T, Kim T K, Cacho C and Hoesch M 2019 Buried double CuO chains in YBa2Cu4O8 uncovered by nano-ARPES *Phys Rev B* **99**
[93] Zhao Y B, Li Y, Chen Y, Chen Y H, Zhou D Q and Zhao Z Q 2020 Ion implantation assisted synthesis of graphene on various dielectric substrates *Nano Res*
[94] Sundarayya Y, Mishra A K, Brand R A, Hahn H, Bansal C and Sunandana C S 2013 Magnetic phase transition and relaxation effects in lithium iron phosphate *Phys Status Solidi B* **250** 1599–605
[95] Yelgel C 2016 Electronic structure of ABC-stacked multilayer graphene and trigonal warping: A first principles calculation *Journal of Physics: Conference Series* 012022
[96] Meng S J, Shi H Y, Sun X D and Gao B 2020 Tuning ultrafast charge carrier dynamics of monolayer graphene using substrates *J Phys Chem C* **124** 21147–54
[97] Khademi A, Sajadi E, Dosanjh P, Bonn D A, Folk J A, Stohr A, Starke U and Forti S 2016 Alkali doping of graphene: The crucial role of high-temperature annealing *Phys Rev B* **94**
[98] Wang Y N, Zhang L, Yang W, Lv S S, Su C H, Xiao H, Zhang F Y, Sui Q M, Jia L and Jiang M S 2020 An in situ reflectance spectroscopic investigation to monitor two-dimensional MoS2 flakes on a sapphire substrate *Materials* **13**
[99] Olimov K, Falk M, Buse K, Woike T, Hormes J and Modrow H 2006 X-ray absorption near edge spectroscopy investigations of valency and lattice occupation site of Fe in highly iron-doped lithium niobate crystals *J Phys-Condens Mat* **18** 5135–46
[100] Qi Y P, Wang Y, Zhang X W, Liu C Q, Hu B B, Bai Y L and Wang X X 2019 A theoretical study of optically enhanced transmission characteristics of subwavelength metal Y-shaped arrays and its application on refractive index sensor *Results Phys* **15**
[101] Liu J Q, Li X L, Han Y D, Wu J B, Zhang X, Wang Z P and Xu Y 2020 Synergetic effect of tetraethylammonium bromide addition on the morphology evolution and enhanced photoluminescence of rare-earth metal-organic frameworks *Inorg Chem* **59** 14318–25
[102] Wu J Y, Chen S C, Do T N, Su W P, Gumbs G and Lin M F 2018 The diverse magneto-optical selection rules in bilayer black phosphorus *Sci Rep-Uk* **8**
[103] Chiu C W, Shyu F L, Chang C P, Chen R B and Lin M F 2003 Optical spectra of AB- and AA-stacked nanographite ribbons *J Phys Soc Jpn* **72** 170–7
[104] Rotenberg E and Bostwick A 2015 Super lattice effects in graphene on SiC(0001) and Ir(111) probed by ARPES *Synthetic Met* **210** 85–94
[105] Trainer D J, Putilov A V, Wang B K, Lane C, Saari T, Chang T R, Jeng H T, Lin H, Xi X X, Nieminen J, Bansil A and Iavarone M 2019 Moire superlattices and 2D electronic properties of graphite/MoS2 heterostructures *J Phys Chem Solids* **128** 325–30
[106] Smirnov D, Schmidt H and Haug R J 2012 Aharonov-Bohm effect in an electron-hole graphene ring system *Appl Phys Lett* **100**
[107] Andrianov A V, Zakhar'in A O, Zhukavin R K, Shastin V N, Abrosimov N V and Bobylev A V 2015 Terahertz intracenter photoluminescence of silicon with lithium at interband excitation *Jetp Lett+* **100** 771–5
[108] Houshmand F, Friedman R, Jalili S and Schofield J 2020 Exciton effect in new generation of carbon nanotubes: Graphdiyne nanotubes *J Mol Model* **26**

[109] Kresse G, Marsman M, Hintzsche L E and Flage-Larsen E 2012 Optical and electronic properties of Si3N4 and alpha-SiO2 *Phys Rev B* **85**
[110] Prakash S, Sharma G and Singh V 2019 Ultra-fast tuning of refractive index in lithium niobate slab by GHz acoustic wave *Optik* **178** 256–62
[111] Torbatian Z, Alidoosti M, Novko D and Asgari R 2020 Low-loss two-dimensional plasmon modes in antimonene *Phys Rev B* **101**
[112] Men N V and Phuong D T K 2020 Plasmon modes in double-layer gapped graphene at zero temperature *Phys Lett A* **384**
[113] Van Men N 2020 Coulomb bare interactions in inhomogeneous 4-layer graphene structures *Phys Lett A* **384**
[114] Novoselov K S, Geim A K, Morozov S V, Jiang D, Katsnelson M I, Grigorieva I V, Dubonos S V and Firsov A A 2005 Two-dimensional gas of massless Dirac fermions in graphene *Nature* **438** 197–200
[115] Kahlert J U, Rawal A, Hook J M, Rendina L M and Choucair M 2014 Carborane functionalization of the aromatic network in chemically-synthesized graphene *Chem Commun* **50** 11332–4
[116] Lee K W and Lee C E 2020 Strain and doping effects on the antiferromagnetism of AB-stacked bilayer silicene *Physica B* **577**
[117] Chen X P, Yang Q, Meng R S, Jiang J K, Liang Q H, Tan C J and Sun X 2016 The electronic and optical properties of novel germanene and antimonene heterostructures *J Mater Chem C* **4** 5434–41
[118] Novoa-De Leon I C, Johny J, Vazquez-Rodriguez S, Garcia-Gomez N, Carranza-Bernal S, Mendivil I, Shaji S and Sepulveda-Guzman S 2019 Tuning the luminescence of nitrogen-doped graphene quantum dots synthesized by pulsed laser ablation in liquid and their use as a selective photoluminescence on-off-on probe for ascorbic acid detection *Carbon* **150** 455–64
[119] Parvaiz M S, Shah K A, Dar G N, Chowdhury S, Farinre O and Misra P 2020 Electronic transport in penta-graphene nanoribbon devices using carbon nanotube electrodes: A computational study *Nanosyst-Phys Chem M* **11** 176–82
[120] Sathishkumar N, Wu S Y and Chen H T 2020 Charge-modulated/electric-field controlled reversible CO2/H-2 capture and storage on metal-free N-doped penta-graphene *Chem Eng J* **391**
[121] Rajbanshi B, Sarkar S, Mandal B and Sarkar P 2016 Energetic and electronic structure of penta-graphene nanoribbons *Carbon* **100** 118–25
[122] Matos M 2002 Electronic structure of several polytypes of SiC: A study of band dispersion from a semi-empirical approach *Physica B* **324** 15–33
[123] Wickramaratne D, Weston L and Van de Walle C G 2018 Monolayer to bulk properties of hexagonal boron nitride *J Phys Chem C* **122** 25524–9
[124] Wu W Z, Lu P, Zhang Z H and Guo W L 2011 Electronic and magnetic properties and structural stability of BeO sheet and nanoribbons *Acs Appl Mater Inter* **3** 4787–95
[125] Yuan P F, Zhang Z H, Fan Z Q and Qiu M 2017 Electronic structure and magnetic properties of penta-graphene nanoribbons *Phys Chem Chem Phys* **19** 9528–36
[126] Novoselov K S, Geim A K, Morozov S V, Jiang D, Zhang Y, Dubonos S V, Grigorieva I V and Firsov A A 2004 Electric field effect in atomically thin carbon films *Science* **306** 666–9
[127] Geim A K 2012 Graphene prehistory *Phys Scripta* **T146**
[128] Zhang C and Liu T X 2012 A review on hybridization modification of graphene and its polymer nanocomposites *Chinese Sci Bull* **57** 3010–21
[129] Ahuja R, Auluck S, Trygg J, Wills J M, Eriksson O and Johansson B 1995 Electronic-structure of graphite—effect of hydrostatic-pressure *Phys Rev B* **51** 4813–19

[130] Li K Y, Eres G, Howe J, Chuang Y J, Li X F, Gu Z J, Zhang L T, Xie S S and Pan Z W 2013 Self-assembly of graphene on carbon nanotube surfaces *Sci Rep-Uk* **3**
[131] Wu Z S, Ren W C, Gao L B, Liu B L, Zhao J P and Cheng H M 2010 Efficient synthesis of graphene nanoribbons sonochemically cut from graphene sheets *Nano Res* **3** 16–22
[132] Tang C, Oppenheim T, Tung V C and Martini A 2013 Structure-stability relationships for graphene-wrapped fullerene-coated carbon nanotubes *Carbon* **61** 458–66
[133] Kariyado T and Hatsugai Y 2015 Manipulation of Dirac cones in mechanical graphene *Sci Rep-Uk* **5**
[134] Phiri J, Johansson L S, Gane P and Maloney T 2018 A comparative study of mechanical, thermal and electrical properties of graphene-, graphene oxide- and reduced graphene oxide-doped microfibrillated cellulose nanocomposites *Compos Part B-Eng* **147** 104–13
[135] Han T H, Kim H, Kwon S J and Lee T W 2017 Graphene-based flexible electronic devices *Mat Sci Eng R* **118** 1–43
[136] Wassei J K and Kaner R B 2010 Graphene, a promising transparent conductor *Mater Today* **13** 52–9
[137] Zhang F, Zhang T F, Yang X, Zhang L, Leng K, Huang Y and Chen Y S 2013 A high-performance supercapacitor-battery hybrid energy storage device based on graphene-enhanced electrode materials with ultrahigh energy density *Energ Environ Sci* **6** 1623–32
[138] Sahu S and Rout G C 2017 Band gap opening in graphene: A short theoretical study *Int Nano Lett* **7** 81–9
[139] Xu X Z, Liu C, Sun Z H, Cao T, Zhang Z H, Wang E G, Liu Z F and Liu K H 2018 Interfacial engineering in graphene band gap *Chem Soc Rev* **47** 3059–99
[140] Fan X F, Shen Z X, Liu A Q and Kuo J L 2012 Band gap opening of graphene by doping small boron nitride domains *Nanoscale* **4** 2157–65
[141] Gui G, Li J and Zhong J X 2008 Band structure engineering of graphene by strain: First-principles calculations *Phys Rev B* **78**
[142] Tang S B, Wu W H, Xie X J, Li X K and Gu J J 2017 Band gap opening of bilayer graphene by graphene oxide support doping *Rsc Adv* **7** 9862–71
[143] Villamagua L, Carini M, Stashans A and Gomez C V 2016 Band gap engineering of graphene through quantum confinement and edge distortions *Ric Mat* **65** 579–84
[144] Iyakutti K, Kumar E M, Thapa R, Rajeswarapalanichamy R, Surya V J and Kawazoe Y 2016 Effect of multiple defects and substituted impurities on the band structure of graphene: A DFT study *J Mater Sci-Mater El* **27** 12669–79
[145] Mak K F, Lui C H, Shan J and Heinz T F 2009 Observation of an electric-field-induced band gap in bilayer graphene by infrared spectroscopy *Phys Rev Lett* **102**
[146] Oughaddou H, Enriquez H, Tchalala M R, Yildirim H, Mayne A J, Bendounan A, Dujardin G, Ali M A and Kara A 2015 Silicene, a promising new 2D material *Prog Surf Sci* **90** 46–83
[147] Acun A, Zhang L, Bampoulis P, Farmanbar M, van Houselt A, Rudenko A N, Lingenfelder M, Brocks G, Poelsema B, Katsnelson M I and Zandvliet H J W 2015 Germanene: The germanium analogue of graphene *J Phys-Condens Mat* **27**
[148] Zhu F F, Chen W J, Xu Y, Gao C L, Guan D D, Liu C H, Qian D, Zhang S C and Jia J F 2015 Epitaxial growth of two-dimensional stanene *Nat Mater* **14** 1020–5
[149] Khandelwal A, Mani K, Karigerasi M H and Lahiri I 2017 Phosphorene—the two-dimensional black phosphorous: Properties, synthesis and applications *Mater Sci Eng B-Adv* **221** 17–34
[150] Singh D, Gupta S K, Sonvane Y and Lukacevic I 2016 Antimonene: A monolayer material for ultraviolet optical nanodevices *J Mater Chem C* **4** 6386–90

[151] Akturk E, Akturk O U and Ciraci S 2016 Single and bilayer bismuthene: Stability at high temperature and mechanical and electronic properties *Phys Rev B* **94**
[152] Manzeli S, Ovchinnikov D, Pasquier D, Yazyev O V and Kis A 2017 2D transition metal dichalcogenides *Nat Rev Mater* **2**
[153] Moore J E 2010 The birth of topological insulators *Nature* **464** 194–8
[154] Saraci F, Quezada-Novoa V, Donnarumma P R and Howarth A J 2020 Rare-earth metal-organic frameworks: From structure to applications *Chem Soc Rev* **49** 7949–77
[155] Gogotsi Y and Anasori B 2019 The rise of MXenes *Acs Nano* **13** 8491–4
[156] Akbari E, Buntat Z, Afroozeh A, Pourmand S E, Farhang Y and Sanati P 2016 Silicene and graphene nano materials in gas sensing mechanism *Rsc Adv* **6** 81647–53
[157] Kharadi M A, Malik G F A, Khanday F A, Shah K R A, Mittal S and Kaushik B K 2020 Review-silicene: From material to device applications *Ecs J Solid State Sc* **9**
[158] Meng L, Wang Y L, Zhang L Z, Du S X, Wu R T, Li L F, Zhang Y, Li G, Zhou H T, Hofer W A and Gao H J 2013 Buckled silicene formation on Ir(111) *Nano Lett* **13** 685–90
[159] Fleurence A, Friedlein R, Ozaki T, Kawai H, Wang Y and Yamada-Takamura Y 2012 Experimental evidence for epitaxial silicene on diboride thin films *Phys Rev Lett* **108**
[160] Vogt P, De Padova P, Quaresima C, Avila J, Frantzeskakis E, Asensio M C, Resta A, Ealet B and Le Lay G 2012 Silicene: Compelling experimental evidence for graphene like two-dimensional silicon *Phys Rev Lett* **108**
[161] Takeda K and Shiraishi K 1994 Theoretical possibility of stage corrugation in Si and Ge analogs of graphite *Phys Rev B* **50** 14916–22
[162] Lima M P, Fazzio A and da Silva A J R 2018 Silicene-based FET for logical technology *Ieee Electr Device L* **39** 1258–61
[163] Aghaei S M, Monshi M M and Calizo I 2016 A theoretical study of gas adsorption on silicene nanoribbons and its application in a highly sensitive molecule sensor *Rsc Adv* **6** 94417–28
[164] Galashev A Y and Ivanichkina K A 2020 Silicene anodes for Lithium-Ion batteries on metal substrates *J Electrochem Soc* **167**
[165] Ye M, Quhe R, Zheng J X, Ni Z Y, Wang Y Y, Yuan Y K, Tse G, Shi J J, Gao Z X and Lu J 2014 Tunable band gap in germanene by surface adsorption *Physica E* **59** 60–5
[166] Nakano H, Tetsuka H, Spencer M J S and Morishita T 2018 Chemical modification of group IV graphene analogs *Sci Technol Adv Mat* **19** 76–100
[167] Aghaei S M and Calizo I 2015 Band gap tuning of armchair silicene nanoribbons using periodic hexagonal holes *J Appl Phys* **118**
[168] Jia T T, Zheng M M, Fan X Y, Su Y, Li S J, Liu H Y, Chen G and Kawazoe Y 2015 Band gap on/off switching of silicene superlattice *J Phys Chem C* **119** 20747–54
[169] Drummond N D, Zolyomi V and Fal'ko V I 2012 Electrically tunable band gap in silicene *Phys Rev B* **85**
[170] Aghaei S M, Torres I and Calizo I 2016 Structural stability of functionalized silicene nanoribbons with normal, reconstructed, and hybrid edges *J Nanomater* **2016**
[171] Chegel R and Hasani M 2020 Electronic and thermal properties of silicene nanoribbons: Third nearest neighbor tight binding approximation *Chem Phys Lett* **761**
[172] De Padova P, Kubo O, Olivieri B, Quaresima C, Nakayama T, Aono M and Le Lay G 2012 Multilayer silicene nanoribbons *Nano Lett* **12** 5500–3
[173] van den Broek B, Houssa M, Lu A, Pourtois G, Afanas'ev V and Stesmans A 2016 Silicene nanoribbons on transition metal dichalcogenide substrates: Effects on electronic structure and ballistic transport *Nano Res* **9** 3394–406
[174] Quertite K, Enriquez H, Trcera N, Tong Y F, Bendounan A, Mayne A J, Dujardin G, Lagarde P, El Kenz A, Benyoussef A, Dappe Y J, Kara A and Oughaddou H 2021 Silicene nanoribbons on an insulating thin film *Adv Funct Mater* **31**

[175] Li H, Wang L, Liu Q H, Zheng J X, Mei W N, Gao Z X, Shi J J and Lu J 2012 High performance silicene nanoribbon field effect transistors with current saturation *Eur Phys J B* **85**
[176] Chen A B, Wang X F, Vasilopoulos P, Zhai M X and Liu Y S 2014 Spin-dependent ballistic transport properties and electronic structures of pristine and edge-doped zigzag silicene nanoribbons: Large magnetoresistance *Phys Chem Chem Phys* **16** 5113–18
[177] Yao Y, Liu A P, Bai J H, Zhang X M and Wang R 2016 Electronic structures of silicene nanoribbons: Two-edge-chemistry modification and first-principles study *Nanoscale Res Lett* **11**
[178] Deng X Q and Sheng R Q 2019 Spin transport investigation of two type silicene nanoribbons heterostructure *Phys Lett A* **383** 47–53
[179] An R L, Wang X F, Vasilopoulos P, Liu Y S, Chen A B, Dong Y J and Zhai M X 2014 Vacancy effects on electric and thermoelectric properties of zigzag silicene nanoribbons *J Phys Chem C* **118** 21339–46
[180] Fang D Q, Zhang Y and Zhang S L 2014 Silicane nanoribbons: Electronic structure and electric field modulation *New J Phys* **16**
[181] Shen M, Zhang Y Y, An X T, Liu J J and Li S S 2014 Valley polarization in graphene-silicene-graphene heterojunction in zigzag nanoribbon *J Appl Phys* **115**
[182] Lu D B, Song Y L, Huang X Y and Wang C 2018 Optical properties of a single carbon chain-doped silicene nanoribbon *J Electron Mater* **47** 4585–93
[183] Zheng F B, Zhang C W, Yan S S and Li F 2013 Novel electronic and magnetic properties in N or B doped silicene nanoribbons *J Mater Chem C* **1** 2735–43
[184] Xu R F, Han K and Li H P 2018 Effect of isotope doping on phonon thermal conductivity of silicene nanoribbons: A molecular dynamics study *Chinese Phys B* **27**
[185] Ma L, Zhang J M, Xu K W and Ji V 2014 Nitrogen and Boron substitutional doped zigzag silicene nanoribbons: Ab initio investigation *Physica E* **60** 112–17
[186] Zhang J M, Song W T, Xu K W and Ji V 2014 The study of the P doped silicene nanoribbons with first-principles *Comp Mater Sci* **95** 429–34
[187] Austin J, Way E M, Jacobberger R M, Goeltl F, Saraswat V, Mavrikakis M and Arnold M S 2019 Tightly Pitched Sub-10 Nm Nanoribbons Grown Via Seeded Anisotropic Synthesis on Ge(001) *ECS Meeting Abstracts*
[188] Hell M G, Senkovskiy B V, Fedorov A V, Nefedov A, Woll C and Gruneis A 2016 Facile preparation of Au(111)/mica substrates for high-quality graphene nanoribbon synthesis *Phys Status Solidi B* **253** 2362–5
[189] Jacobse P H, Kimouche A, Gebraad T, Ervasti M M, Thijssen M, Liljeroth P and Swart I 2017 Electronic components embedded in a single graphene nanoribbon *Nat Commun* **8**
[190] Owens F J 2008 Electronic and magnetic properties of armchair and zigzag graphene nanoribbons *J Chem Phys* **128**
[191] Singh S and Kaur I 2020 Band gap engineering in armchair graphene nanoribbon of zigzag-armchair-zigzag based nano-FET: A DFT investigation *Physica E* **118**
[192] Han M Y, Ozyilmaz B, Zhang Y B and Kim P 2007 Energy band-gap engineering of graphene nanoribbons *Phys Rev Lett* **98**
[193] Bai J W, Duan X F and Huang Y 2009 Rational fabrication of graphene nanoribbons using a nanowire etch mask *Nano Lett* **9** 2083–7
[194] Wang X R, Ouyang Y J, Li X L, Wang H L, Guo J and Dai H J 2008 Room-temperature all-semiconducting sub-10-nm graphene nanoribbon field-effect transistors *Phys Rev Lett* **100**
[195] Fujii S and Enoki T 2010 Cutting of oxidized graphene into nanosized pieces *J Am Chem Soc* **132** 10034–41
[196] Sprinkle M, Ruan M, Hu Y, Hankinson J, Rubio-Roy M, Zhang B, Wu X, Berger C and de Heer W A 2010 Scalable templated growth of graphene nanoribbons on SiC *Nat Nanotechnol* **5** 727–31

[197] Jiao L Y, Xie L M and Dai H J 2012 Densely aligned graphene nanoribbons at similar to 35 nm pitch *Nano Res* **5** 292–6
[198] Li X L, Wang X R, Zhang L, Lee S W and Dai H J 2008 Chemically derived, ultrasmooth graphene nanoribbon semiconductors *Science* **319** 1229–32
[199] Lin J, Raji A R O, Nan K W, Peng Z W, Yan Z, Samuel E L G, Natelson D and Tour J M 2014 Iron oxide nanoparticle and graphene nanoribbon composite as an anode material for high-performance li-ion batteries *Adv Funct Mater* **24** 2044–8
[200] Li Y S, Ao X, Liao J L, Jiang J J, Wang C D and Chiang W H 2017 Sub-10-nm graphene nanoribbons with tunable surface functionalities for lithium-ion batteries *Electrochim Acta* **249** 404–12
[201] Zou X L, Wang L Q and Yakobson B I 2018 Mechanisms of the oxygen reduction reaction on B- and/or N-doped carbon nanomaterials with curvature and edge effects *Nanoscale* **10** 1129–34
[202] Chang S L, Wu B R, Yang P H and Lin M F 2012 Curvature effects on electronic properties of armchair graphene nanoribbons without passivation *Phys Chem Chem Phys* **14** 16409–14
[203] Wang Y, Zhan H F, Yang C, Xiang Y and Zhang Y Y 2015 Formation of carbon nanoscrolls from graphene nanoribbons: A molecular dynamics study *Comp Mater Sci* **96** 300–5
[204] Kawai S, Saito S, Osumi S, Yamaguchi S, Foster A S, Spijker P and Meyer E 2015 Atomically controlled substitutional boron-doping of graphene nanoribbons *Nat Commun* **6**
[205] Nguyen D K, Tran N T T, Nguyen T T and Lin M F 2018 Diverse electronic and magnetic properties of chlorination-related graphene nanoribbons *Sci Rep-Uk* **8**
[206] Huang Y C, Chang C P and Lin M F 2007 Magnetic and quantum confinement effects on electronic and optical properties of graphene ribbons *Nanotechnology* **18**
[207] Son Y W, Cohen M L and Louie S G 2006 Half-metallic graphene nanoribbons *Nature* **444** 347–9
[208] Iijima S 1991 Helical microtubules of graphitic carbon *Nature* **354** 56–8
[209] Deheer W A, Bacsa W S, Chatelain A, Gerfin T, Humphreybaker R, Forro L and Ugarte D 1995 Aligned carbon nanotube films—production and optical and electronic-properties *Science* **268** 845–7
[210] Liu J, Dai H J, Hafner J H, Colbert D T, Smalley R E, Tans S J and Dekker C 1997 Fullerene "crop circles" *Nature* **385** 780–1
[211] Thess A, Lee R, Nikolaev P, Dai H J, Petit P, Robert J, Xu C H, Lee Y H, Kim S G, Rinzler A G, Colbert D T, Scuseria G E, Tomanek D, Fischer J E and Smalley R E 1996 Crystalline ropes of metallic carbon nanotubes *Science* **273** 483–7
[212] Ren Z F, Huang Z P, Xu J W, Wang J H, Bush P, Siegal M P and Provencio P N 1998 Synthesis of large arrays of well-aligned carbon nanotubes on glass *Science* **282** 1105–7
[213] Fan S S, Chapline M G, Franklin N R, Tombler T W, Cassell A M and Dai H J 1999 Self-oriented regular arrays of carbon nanotubes and their field emission properties *Science* **283** 512–14
[214] Rao A M, Richter E, Bandow S, Chase B, Eklund P C, Williams K A, Fang S, Subbaswamy K R, Menon M, Thess A, Smalley R E, Dresselhaus G and Dresselhaus M S 1997 Diameter-selective Raman scattering from vibrational modes in carbon nanotubes *Science* **275** 187–91
[215] Cowley J M, Nikolaev P, Thess A and Smalley R E 1997 Electron nano-diffraction study of carbon single-walled nanotube ropes *Chem Phys Lett* **265** 379–84
[216] Wildoer J W G, Venema L C, Rinzler A G, Smalley R E and Dekker C 1998 Electronic structure of atomically resolved carbon nanotubes *Nature* **391** 59–62

[217] Odom T W, Huang J L, Kim P and Lieber C M 1998 Atomic structure and electronic properties of single-walled carbon nanotubes *Abstr Pap Am Chem S* **216** U77–8
[218] Kataura H, Kumazawa Y, Maniwa Y, Umezu I, Suzuki S, Ohtsuka Y and Achiba Y 1999 Optical properties of single-wall carbon nanotubes *Synthetic Met* **103** 2555–8
[219] Jost O, Gorbunov A A, Pompe W, Pichler T, Friedlein R, Knupfer M, Reibold M, Bauer H D, Dunsch L, Golden M S and Fink J 1999 Diameter grouping in bulk samples of single-walled carbon nanotubes from optical absorption spectroscopy *Appl Phys Lett* **75** 2217–19
[220] Bursill L A, Stadelmann P A, Peng J L and Prawer S 1994 Surface-plasmon observed for carbon nanotubes *Phys Rev B* **49** 2882–7
[221] Burghard M, Klauk H and Kern K 2009 Carbon-based field-effect transistors for nano-electronics *Adv Mater* **21** 2586–600
[222] Tans S J, Verschueren A R M and Dekker C 1998 Room-temperature transistor based on a single carbon nanotube *Nature* **393** 49–52
[223] Martel R, Schmidt T, Shea H R, Hertel T and Avouris P 1998 Single- and multi-wall carbon nanotube field-effect transistors *Appl Phys Lett* **73** 2447–9
[224] Schmidt O G and Eberl K 2001 Nanotechnology—Thin solid films roll up into nanotubes *Nature* **410** 168
[225] Jeong S Y, Kim J Y, Yang H D, Yoon B N, Choi S H, Kang H K, Yang C W and Lee Y H 2003 Synthesis of silicon nanotubes on porous alumina using molecular beam epitaxy *Adv Mater* **15** 1172–6
[226] De Crescenzi M, Castrucci P, Scarselli M, Diociaiuti M, Chaudhari P S, Balasubramanian C, Bhave T M and Bhoraskar S V 2005 Experimental imaging of silicon nanotubes *Appl Phys Lett* **86**
[227] Yari H, Pakizeh M and Namvar-Mahboub M 2019 Effect of silica nanotubes on characteristic and performance of PVDF nanocomposite membrane for nitrate removal application *J Nanopart Res* **21**
[228] Kasavajjula U, Wang C S and Appleby A J 2007 Nano- and bulk-silicon-based insertion anodes for lithium-ion secondary cells *J Power Sources* **163** 1003–39
[229] Zhu J, Yu Z F, Burkhard G F, Hsu C M, Connor S T, Xu Y Q, Wang Q, McGehee M, Fan S H and Cui Y 2009 Optical absorption enhancement in amorphous silicon nanowire and nanocone arrays *Nano Lett* **9** 279–82
[230] Feng K, Li M, Liu W W, Kashkooli A G, Xiao X C, Cai M and Chen Z W 2018 Silicon-based anodes for lithium-ion batteries: From fundamentals to practical applications *Small* **14**
[231] Miyake T and Saito S 2003 Quasiparticle band structure of carbon nanotubes *Phys Rev B* **68**
[232] Kane C L and Mele E J 1997 Size, shape, and low energy electronic structure of carbon nanotubes *Phys Rev Lett* **78** 1932–5
[233] Shyu F L and Lin M F 2002 Electronic and optical properties of narrow-gap carbon nanotubes *J Phys Soc Jpn* **71** 1820–3
[234] Zhao H, Zhang C W, Ji W X, Zhang R W, Li S S, Yan S S, Zhang B M, Li P and Wang P J 2016 Unexpected giant-gap quantum spin hall insulator in chemically decorated plumbene monolayer *Sci Rep-Uk* **6**
[235] Yuhara J, He B J, Matsunami N, Nakatake M and Le Lay G 2019 Graphene's latest cousin: Plumbene epitaxial growth on a "Nano WaterCube" *Adv Mater* **31**
[236] Elias D C, Nair R R, Mohiuddin T M G, Morozov S V, Blake P, Halsall M P, Ferrari A C, Boukhvalov D W, Katsnelson M I, Geim A K and Novoselov K S 2009 Control of graphene's properties by reversible hydrogenation: Evidence for graphane *Science* **323** 610–13

[237] Pumera M and Wong C H A 2013 Graphane and hydrogenated graphene *Chem Soc Rev* **42** 5987–95
[238] Brownson D A C and Banks C E 2010 Graphene electrochemistry: An overview of potential applications *Analyst* **135** 2768–78
[239] Abergel D S L, Apalkov V, Berashevich J, Ziegler K and Chakraborty T 2010 Properties of graphene: A theoretical perspective *Adv Phys* **59** 261–482
[240] Geim A K and MacDonald A H 2007 Graphene: Exploring carbon flatland *Phys Today* **60** 35–41
[241] Nakamura D, Suzumura A and Shigetoh K 2015 Sintered tantalum carbide coatings on graphite substrates: Highly reliable protective coatings for bulk and epitaxial growth *Appl Phys Lett* **106**
[242] Ho J H, Lu C L, Hwang C C, Chang C P and Lin M F 2006 Coulomb excitations in AA- and AB-stacked bilayer graphites *Phys Rev B* **74**
[243] Ling C Y, Lee M H and Lin M F 2018 Coulomb excitations in ABC-stacked trilayer graphene *Phys Rev B* **98**
[244] Shallcross S, Sharma S, Kandelaki E and Pankratov O A 2010 Electronic structure of turbostratic graphene *Phys Rev B* **81**
[245] Zhang F, Jia L Q, Sun X T, Dai X Q, Huang Q X and Li W 2020 Tuning Schottky barrier in graphene/InSe van der Waals heterostructures by electric field *Acta Phys Sin-Ch Ed* **69**
[246] Eklund P C 1981 Optical studies of the electronic and lattice dynamical properties of graphite-intercalation compounds *B Am Phys Soc* **26** 265
[247] Xu J T, Dou Y H, Wei Z X, Ma J M, Deng Y H, Li Y T, Liu H K and Dou S X 2017 Recent progress in graphite intercalation compounds for rechargeable metal (Li, Na, K, Al)-Ion batteries *Adv Sci* **4**
[248] Meng X Q, Tongay S, Kang J, Chen Z H, Wu F M, Li S S, Xia J B, Li J B and Wu J Q 2013 Stable p- and n-type doping of few-layer graphene/graphite *Carbon* **57** 507–14
[249] Toyoura K, Koyama Y, Kuwabara A, Oba F and Tanaka I 2008 First-principles approach to chemical diffusion of lithium atoms in a graphite intercalation compound *Phys Rev B* **78**
[250] Marinopoulos A G, Reining L, Rubio A and Olevano V 2004 Ab initio study of the optical absorption and wave-vector-dependent dielectric response of graphite *Phys Rev B* **69**
[251] Ryu Y K, Frisenda R and Castellanos-Gomez A 2019 Superlattices based on van der Waals 2D materials *Chem Commun* **55** 11498–510
[252] Gao Y R, Zhu C Q, Chen Z Z and Lu G 2017 Understanding ultrafast rechargeable aluminum-ion battery from first-principles *J Phys Chem C* **121** 7131–8
[253] Dresselhaus G and Leung S Y 1981 Phenomenological model for the electronic-structure of graphite-intercalation compounds *Physica B & C* **105** 495–500
[254] Christensen J, Albertus P, Sanchez-Carrera R S, Lohmann T, Kozinsky B, Liedtke R, Ahmed J and Kojic A 2011 A critical review of li/air batteries *Journal of the Electrochemical Society* **159** R1
[255] Pistoia G 2013 *Lithium-Ion Batteries* (Amsterdam: Elsevier)
[256] Yoshio M, Brodd R J and Kozawa A 2009 *Lithium-Ion Batteries* vol 1 (Berlin: Springer)
[257] Xu M S, Liang T, Shi M M and Chen H Z 2013 Graphene-like two-dimensional materials *Chemical Reviews* **113** 3766–98
[258] Kim S Y, Kwak J, Ciobanu C V and Kwon S Y 2019 Recent developments in controlled vapor-phase growth of 2D group 6 transition metal dichalcogenides *Adv Mater* **31**
[259] Liu G B, Xiao D, Yao Y G, Xu X D and Yao W 2015 Electronic structures and theoretical modelling of two-dimensional group-VIB transition metal dichalcogenides *Chemical Society Reviews* **44** 2643–63

[260] Xia J, Yan J X and Shen Z X 2017 Transition metal dichalcogenides: Structural, optical and electronic property tuning via thickness and stacking *Flatchem* **4** 1–19
[261] Puretzky A A, Liang L B, Li X F, Xiao K, Sumpter B G, Meunier V and Geohegan D B 2016 Twisted MoSe2 bilayers with variable local stacking and interlayer coupling revealed by low-frequency Raman spectroscopy *Acs Nano* **10** 2736–44
[262] Samad L, Bladow S M, Ding Q, Zhuo J Q, Jacobberger R M, Arnold M S and Jin S 2016 Layer-controlled chemical vapor deposition growth of MoS2 vertical heterostructures via van der Waals epitaxy *Acs Nano* **10** 7039–46
[263] Ye H, Zhou J D, Er D Q, Price C C, Yu Z Y, Liu Y M, Lowengrub J, Lou J, Liu Z and Shenoy V B 2017 Toward a mechanistic understanding of vertical growth of van der Waals stacked 2D materials: A multiscale model and experiments *Acs Nano* **11** 12780–8
[264] He Y M, Sobhani A, Lei S D, Zhang Z H, Gong Y J, Jin Z H, Zhou W, Yang Y C, Zhang Y, Wang X F, Yakobson B, Vajtai R, Halas N J, Li B, Xie E Q and Ajayan P 2016 Layer engineering of 2D semiconductor junctions *Advanced Materials* **28** 5126–32
[265] Kim S, Konar A, Hwang W S, Lee J H, Lee J, Yang J, Jung C, Kim H, Yoo J B, Choi J Y, Jin Y W, Lee S Y, Jena D, Choi W and Kim K 2012 High-mobility and low-power thin-film transistors based on multilayer MoS2 crystals *Nature Communications* **3**
[266] Liu X C, Qu D S, Ryu J J, Ahmed F, Yang Z, Lee D Y and Yoo W J 2016 P-type polar transition of chemically doped multilayer MoS2 transistor *Advanced Materials* **28** 2345–51
[267] Li H, Yin Z Y, He Q Y, Li H, Huang X, Lu G, Fam D W H, Tok A I Y, Zhang Q and Zhang H 2012 Fabrication of single- and multilayer MoS2 film-based field-effect transistors for sensing NO at room temperature *Small* **8** 63–7
[268] Das S, Chen H Y, Penumatcha A V and Appenzeller J 2013 High performance multilayer MoS2 transistors with scandium contacts *Nano Letters* **13** 100–5
[269] Yan A, Ong C S, Qiu D Y, Ophus C, Ciston J, Merino C, Louie S G and Zettl A 2017 Dynamics of symmetry-breaking stacking boundaries in bilayer MoS2 *The Journal of Physical Chemistry C* **121** 22559–66
[270] Nalin Mehta A, Gauquelin N, Nord M, Orekhov A, Bender H, Cerbu D, Verbeeck J and Vandervorst W 2020 Unravelling stacking order in epitaxial bilayer MX2 using 4D-STEM with unsupervised learning *Nanotechnology* **31** 445702
[271] Zeng F, Zhang W-B and Tang B-Y 2015 Electronic structures and elastic properties of monolayer and bilayer transition metal dichalcogenides MX_2 (M = Mo, W; X = O, S, Se, Te): A comparative first-principles study *Chinese Physics B* **24**
[272] Wang Y, Cong C, Shang J, Eginligil M, Jin Y, Li G, Chen Y, Peimyoo N and Yu T 2019 Unveiling exceptionally robust valley contrast in AA- and AB-stacked bilayer WS2 *Nanoscale Horiz* **4** 396–403
[273] Kanazawa T, Amemiya T, Ishikawa A, Upadhyaya V, Tsuruta K, Tanaka T and Miyamoto Y 2016 Few-layer HfS2 transistors *Scientific Reports* **6**
[274] Ding G Q, Gao G Y, Huang Z S, Zhang W X and Yao K L 2016 Thermoelectric properties of monolayer MSe2 (M = Zr, Hf): Low lattice thermal conductivity and a promising figure of merit *Nanotechnology* **27**
[275] Yin L, Xu K, Wen Y, Wang Z X, Huang Y, Wang F, Shifa T A, Cheng R, Ma H and He J 2016 Ultrafast and ultrasensitive phototransistors based on few-layered HfSe2 *Applied Physics Letters* **109**
[276] Xu K, Wang Z X, Wang F, Huang Y, Wang F M, Yin L, Jiang C and He J 2015 Ultrasensitive phototransistors based on few-layered HfS2 *Advanced Materials* **27** 7881–7
[277] Yan P, Gao G Y, Ding G Q and Qin D 2019 Bilayer MSe2 (M= Zr, Hf) as promising two-dimensional thermoelectric materials: A first-principles study *Rsc Advances* **9** 12394–403